Worcester Polytechnic Institute

Mechanical Engineering Department

Major Qualifying Project

Final Report

Switch-Mode CVT: Torsion Spring

Thursday, April 28, 2011

Submitted by

Michael S. Collins **Matthew A. Rotier** **Scott R. Woodnorth**

Approved by

Professor James D. Van de Ven

Abstract

A Switch-Mode Continuously Variable Transmission is the mechanical analog of a boost converter circuit. The system uses a high-speed clutch to transfer packets of energy from a flywheel to a torsion spring, which drives the output. This project focuses on the design of a torsion spring, which can deflect 180 deg., has a linear spring rate, and fits into a car transmission. It must also have low inertia, to ensure efficiency, and be back-drivable, for regenerative braking. Two unique designs were prototyped then tested using a simulated drive-train consisting of a flywheel input, an electromagnetic clutch, and a disc brake or flywheel. By comparing qualitative and quantitative characteristics of each, the group chose one design which was developed full-scale and tested.

Acknowledgements

The group would like to thank:

- Professor Robert Norton (WPI)
- Dr. Adriana Hera (WPI)
- Neil Whitehouse (WPI)
- Peter Lentros (Lentros Engineering Inc.)
- Professor James Van de Ven (WPI Project Advisor)
- David Collins (off campus machining)

Table of Contents

Abstract ii

Acknowledgements iii

Table of Contents iv

List of Figures vii

List of Tables x

Introduction 1

Background 2

- Hybrid Systems 4
- CVT History 6
- Switch-Mode PWM CVT Concept 7
- Torsion Spring 10
- Previous Research 10
- Background Research 11
- Torsion Spring Background 11
- Patents 12
- Helical Torsion Springs 14
- Cams 15

Objectives 17

Design 18

- Initial Designs 18
  - Magnetic Damper 18
  - Cam Separation Spring 20
  - Magnetic Series Spring 20

Helical Spring 21
Wire Spring 22
Rotini Spring 22
Machined Spring 23
Torsion Piston 24
Decision Matrix I 24
Alpha Prototype Designs 25
Cam Separation Spring 25
Series Spring 28
Machined Spring 33
Methodology 34
Testing System Fabrication 34
Virtual Interface 39
System Control 40
Data Collection 42
Testing Procedure 44
Basic Procedures 44
Series Spring 46
Cam Spring 46
Results 47
Round 1 47
Qualitative Results 47
Quantitative Results 48
Round 2 52

Qualitative Results 52
Quantitative Results 52
Conclusions and Recommendations 54
References 57
Appendix 59
Appendix A – Round 1 Plots 59
Cam Spring 59
Series Spring 69
Appendix B – Round 2 Plots 75
Appendix C – Photo Documentation 78

List of Figures

Figure 1: Energy Flow in the US, 2009. (Lawrence Livermore National Laboratories, US DOE) 3
Figure 2: Crude Oil Prices 1947-2009 (Williams, 2007) 3
Figure 3: Energy vs. Power Density of Various Technologies (Baseley et. al., 2007) 5
Figure 4: Toroidal Continuously Variable Transmission (Harris) 6
Figure 5: Switch Mode PWM CVT Concept 7
Figure 6: Electrical Boost Converter Circuit 8
Figure 7: Pulse-Width Modulation Signal (Anonymous, 2010) 9
Figure 8: PWM Signal of Switch-Mode CVT 9
Figure 9: Switch-Mode CVT System and PWM Signal 10
Figure 10: Original Torsion Spring Design (Morocco, Lambusta, DeMalia, & Araujo, 2009) 11
Figure 11: Torsion Spring Type Damper Disc (Takeuchi, 1992) 13
Figure 12: Torsion Spring Design (Jonsson, 1954) 14
Figure 13: Rectangular Cross Section Spring Calculations (SAE International, 1996) 15
Figure 14: Cam Face Force Diagram 16
Figure 15: Magnetic Damper Iteration 1 19
Figure 16: Magnetic Damper Iteration 2 19
Figure 17: Magnetic Damper Iteration 3 19
Figure 18: Open face cam design 20
Figure 19: Magnetic Series Spring Design 21
Figure 20: Machined Spring 23
Figure 21: Mirror Cam Assembly 26
Figure 22: Cam Spring Final Design 28
Figure 23: Torsion Spring Type Damper Disc (Takeuchi, 1992) 29
Figure 24: Series Spring Conceptual Design 30
Figure 25: Series Spring Iteration 2 30
Figure 26: Series Spring Iteration 3 31
Figure 27: Series Spring FEA Analysis 32
Figure 28: Series Spring Iteration 4 32

Figure 29 - Testing Assembly with Cam Spring Prototype Installed 35
Figure 30: Base of Test Assembly (Bottom Side) 37
Figure 31: Safety Enclosure - Profile View 38
Figure 32: Safety Enclosure with Test Stand 38
Figure 33: Testing VI Block Diagram 40
Figure 34: Electromagnetic Clutch Control Circuit 41
Figure 35: Testing VI Front Panel 42
Figure 36: Example Angular Displacement, Velocity, and Acceleration Curves (Cam Spring) 50
Figure 37: Example Angular Displacement, Velocity, and Acceleration Curves (Series Spring) 50
Figure 38: Round 1 (left) and Round 2 (right) Results (600 RPMs and 50% Duty Cycle) 53
Figure 39: Full Scale Cam Spring Prototype 55
Figure 40: Cam Spring Data Set 1.1 59
Figure 41: Cam Spring Data Set 1.2 60
Figure 42: Cam Spring Data Set 1.3 60
Figure 43: Cam Spring Data Set 1.4 61
Figure 44: Cam Spring Data Set 1.5 61
Figure 45: Cam Spring Data Set 1.6 62
Figure 46: Cam Spring Data Set 1.7 62
Figure 47: Cam Spring Data Set 1.8 63
Figure 48: Cam Spring Data Set 1.9 63
Figure 49: Cam Spring Data Set 1.10 64
Figure 50: Cam Spring Data Set 1.11 64
Figure 51: Cam Spring Data Set 1.12 65
Figure 52: Cam Spring Data Set 1.13 65
Figure 53: Cam Spring Data Set 1.14 66
Figure 54: Cam Spring Data Set 1.15 66
Figure 55: Cam Spring Data Set 1.16 67
Figure 56: Cam Spring Data Set 1.17 67
Figure 57: Cam Spring Data Set 1.18 68

Figure 58: Cam Spring Data Set 1.19 68
Figure 59: Series Spring Data Set 1.1 69
Figure 60: Series Spring Data Set 1.2 69
Figure 61: Series Spring Data Set 1.3 70
Figure 62: Series Spring Data Set 1.4 70
Figure 63: Series Spring Data Set 1.5 71
Figure 64: Series Spring Data Set 1.6 71
Figure 65: Series Spring Data Set 1.7 72
Figure 66: Series Spring Data Set 1.8 72
Figure 67: Series Spring Data Set 1.9 73
Figure 68: Series Spring Data Set 1.10 73
Figure 69: Series Spring Data Set 1.11 74
Figure 70: Cam Spring Data Set 2.1 75
Figure 71: Cam Spring Data Set 2.2 76
Figure 72: Series Spring Data Set 2.3 76
Figure 73: Cam Spring Data Set 2.4 77
Figure 74: Cam Spring Data Set 2.5 77
Figure 75: Cam Spring Data Set 2.6 78
Figure 76: NI DAQ Pin Diagram 79
Figure 77: Counter Pin Location List (Used to Wire encoders) 80
Figure 78: NI PCI-6220 Wiring Photo (Hall Effect Sensor) 81
Figure 79: NI PCI 6024E Wiring Photo (Encoders) 82
Figure 80: Final Testing Assembly 83

List of Tables

Table 1: Decision Matrix Round 1 24
Table 2: Mirror Spring Rate Calculations 27
Table 3: Helical Torsion Spring Physical Characteristics 33
Table 4: List of Measurement Devices 35
Table 5: Flywheel Sizing Table 36
Table 6: List of Tests Performed 44

Introduction

The energy consumption of the planet is currently at an all-time high; a large majority of this energy comes from nonrenewable sources. The supply of these nonrenewable fuels such as coal and oil is becoming too low to ignore which is why much research is currently being conducted into making more energy efficient devices. Large improvements in energy economies stand to be made in engine and transmission systems due to their high use and relatively low efficiencies. The most common method for making these devices more efficient is to couple them to an energy storage device and create a hybrid system. Hybrid systems provide efficiency gains because the energy storage device in the assembly serves as a buffer between the engine and the load which allows the engine to operate at peak economy for longer. Standard energy storage technology for hybrid systems includes batteries, hydraulic and pneumatic accumulators, and flywheels.

Flywheels show great potential for use as energy storage in hybrid systems because they have energy density comparable to lithium ion batteries, which are commonly used in hybrid systems, yet have power density which is orders of magnitude greater. Because of their large potential to improve the capability of hybrid systems, flywheels as energy storage technologies are currently being researched at Worcester Polytechnic Institute's Mechanical Energy and Power Systems laboratory.

The concept that this project worked to realize is a pulse-width modulated continuously variable transmission (PWM, CVT) which will be able to efficiently use energy stored in a flywheel. The transmission utilizes a high speed, low slip clutch to produce a PWM signal in an output shaft. The extremely high speed at which the clutch operates, 100 Hz, allows the system to precisely vary the percentage of energy which is being taken from the flywheel at any given time without bringing the flywheel to a complete stop. An accepted effect of using PWM in a mechanical system is that extremely high accelerations and jerks are created in the output shaft by the clutch. These loads, if unchecked, will lead to early fatigue failure in the system. To alleviate this problem, it is necessary to add a torsion spring to the system in order to reduce the acceleration and jerk within the output shaft.

The goal of this project was to design, build, and test a torsion spring prototype for implementation within the PWM CVT system. To achieve this goal, the spring must minimize acceleration and jerk within the system during operation. The prototype must also exhibit high deflection, low moment of inertia, and low energy loss during operation so as to increase efficiency.

In the future, the spring prototype developed by the group will be connected into a concept clutch developed in the MEPS lab and the efficiency of the entire system will be investigated. Because of this, the spring prototype had to meet size and strength constraints as defined by the clutch prototype. Additionally, the spring prototype must be easily scalable as there are many areas of industry where the concept proves useful.

In this report, an overview of the concepts of the problem will be given so that the user may fully understand the problem and concept. The background is followed by the task specifications and subsequently by the methodology of the design, building, and testing processes. The paper then finishes with a discussion of the results observed from testing as well as a recommendations section which outlines areas in which progress could be made.

Background

The modern world is one which is powered primarily with fossil fuels; America is certainly no exception. According to the Lawrence Livermore National Laboratories, the US consumed 78.4 quad btu's of energy in 2009 which accounted for 82.8 percent of all energy consumed during the year (Figure 1). The high use of fossil fuels is easy to explain; they all have relatively high energy densities and are easy to extract. Unfortunately fossil fuels are, by definition, nonrenewable and the world is running out of them. According to Professor Ibrahim Nashawi of Kuwait University, humanity will likely reach a crude oil production limit by 2014 (Nashawi, 2010). The effects of the gasoline shortage have already begun as exhibited by the rapid increase in the cost of crude oil. As Figure 2 shows, the price of crude oil has risen from $20 to almost $100 over the last decade (Williams, 2007). With resources diminishing and the

demand for energy increasing daily, more efficient devices are needed to increase the longevity of this critical resource.

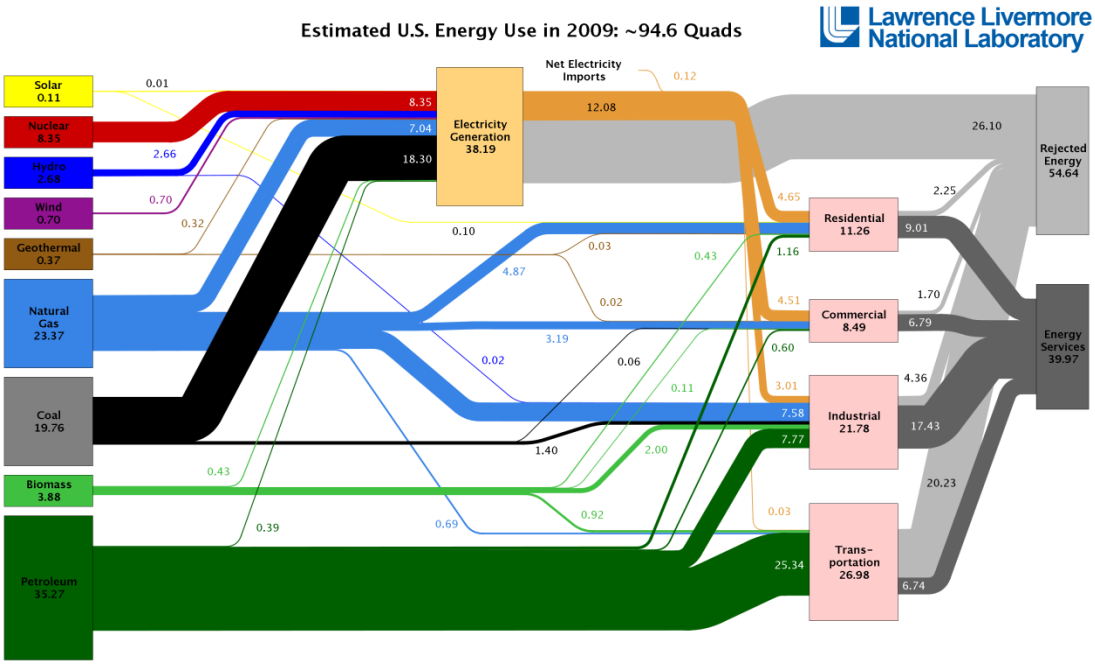

Figure 1: Energy Flow in the US, 2009. (Lawrence Livermore National Laboratories, US DOE)

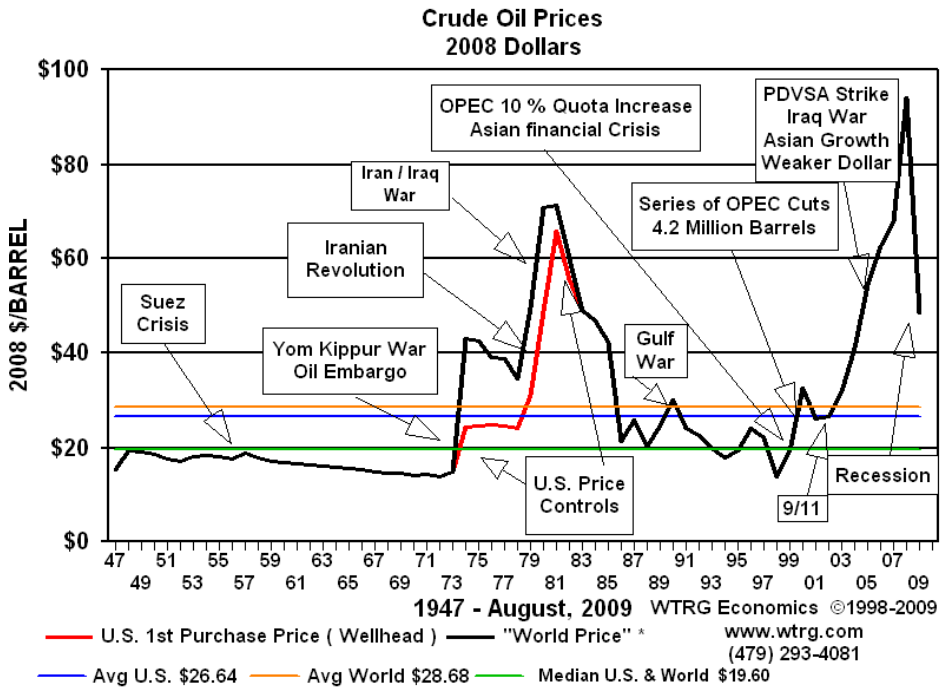

Figure 2: Crude Oil Prices 1947-2009 (Williams, 2007)

One simple method of quickly reducing oil consumption is to simply produce more energy efficient devices. Machines which are energy efficient help reduce the demand on current the current energy infrastructure in the US and also will help ensure that the clean energy produced in the future is used well. One area where implementing more energy economical systems can have an immediate, measureable benefit is mechanical transmissions. Transmissions are used all across industry today anywhere that mechanical power produced by an engine or motor needs to be formatted to work on a load. Current transmissions generally rely on a complex system of gears and couplings in order to convey power but are limited in that they must use finite, predetermined gear ratios during use. Having restricted gearing ratios forces the engine to operate outside of its peak efficiency range often to account for load changes which in turn increases fuel consumption. A simple route to increasing energy efficiency within a system is therefore to produce a transmission system which allows the engine to run in its peak efficiency range for longer. A common way to accomplish this is through hybrid systems.

Hybrid Systems

A hybrid system is one in which an energy storage system is installed in parallel to a standard transmission. The energy storage device increases system efficiency by acting as a buffer between the engine and the load source. If energy demand in a hybrid system is low, the engine can continue operating at a highly efficient rpm as unused energy is simply stored for later. When demand is high, stored energy can be used to alleviate engine load. Further, during braking, hybrid systems can recycle energy normally lost and save it for later. Common energy storage devices used in hybrid systems include batteries, hydraulic accumulators, and flywheels.

Flywheels have great potential for use in hybrid systems but are currently used only sparingly. In terms of energy density, flywheels are orders of magnitude lower than standard gasoline; what they lack in energy density however, flywheels make up for with power density (Figure 3.) More important perhaps than how flywheels perform compared to gasoline, is how they compare to battery energy storage. When compared to lithium ion batteries, the most

common energy storage medium in hybrid systems today, flywheels have comparable energy density per unit mass and still maintain a large advantage in terms of power density. In short, though flywheels do not necessarily have the potential to replace gasoline engines as the primary energy source in mechanical systems, they show very high potential for implementation as energy storage technology in hybrid systems.

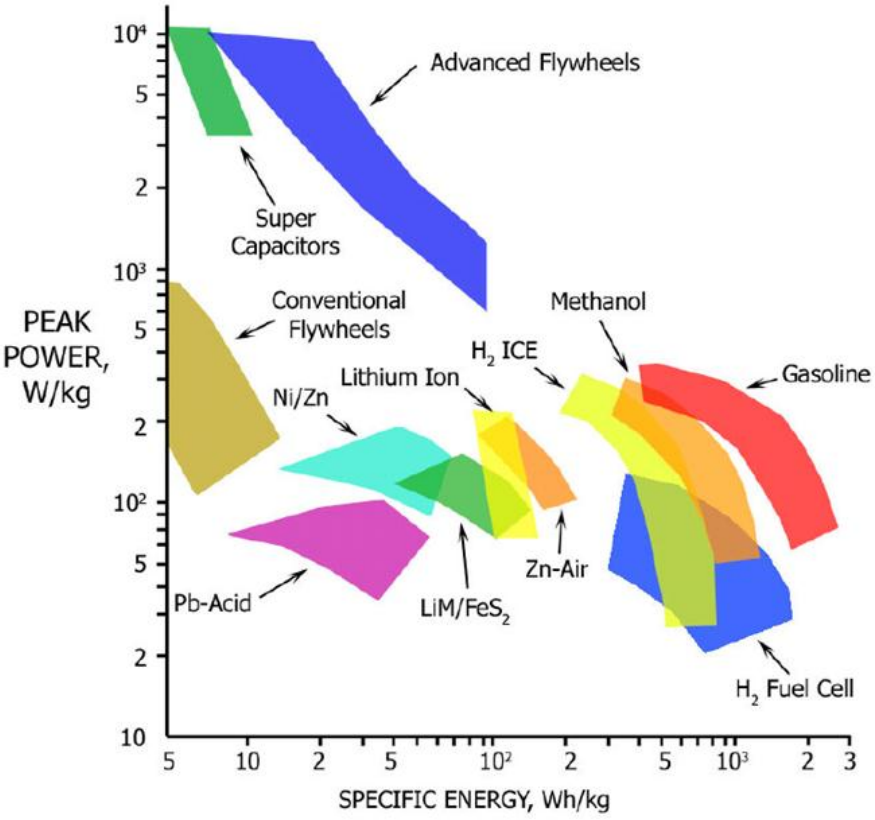

Figure 3: Energy vs. Power Density of Various Technologies (Baseley et. al., 2007)

Although flywheels have a great advantage over batteries, they are used in industry relatively rarely. The reasons for this are simple: flywheels only recently experienced the necessary performance gains to make them viable. These performance gains were primarily in the area of either wheel materials, where carbon fiber allows for extremely high rpm capability, or in improved bearing systems, where extremely low magnetic bearings lower energy leakage overall. (Hebner, Beno, Walls, & University of Texas)

A further reason for the relative rarity of flywheels is because they require complex linkages to match their changing rpm's to an output. Currently, the most common way to insert a flywheel into a hybrid system is through a continuously variable transmission (CVT).

CVT History

Continuously Variable Transmissions (CVT) have been investigated as a means of improving engine efficiency since the Industrial Revolution. The CVT was originally conceptualized by Leonardo da Vinci in 1490 as a "stepless" transmission (Birch, 2010) and, although it is an extremely old idea, still has large potential for growth. The adjective "continuous" is derived from the "stepless" functionality proposed by da Vinci. Although conceptualized early on, CVT's were late to be put into practice. The first patent for a CVT was issued to Daimler and Benz in 1886 for a toroidal CVT (Harris). A toroidal CVT, as shown in Figure 4, consists of an input and an output disc which form an hourglass-like shape and two rollers which rely on friction to transmit energy from one disc to another. By adjusting the angle of the rollers, the input to output ratio of the gear train can be finely controlled which allows drive shaft speed to be decoupled from engine speed, a major aid to overall system efficiency (Harris).

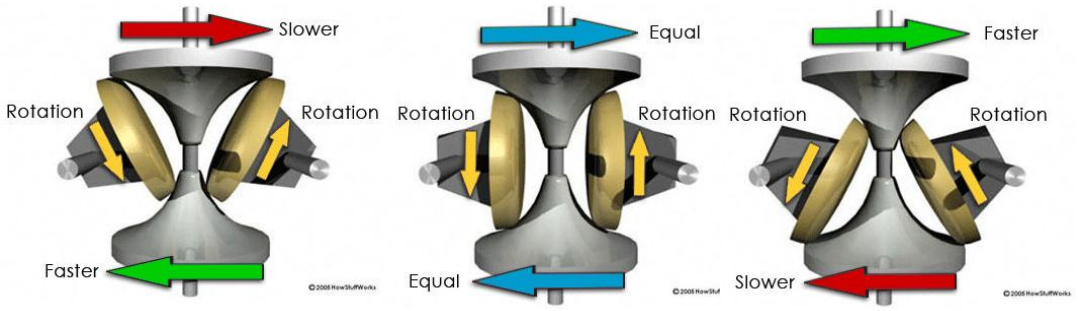

Figure 4: Toroidal Continuously Variable Transmission (Harris)

Continuously variable transmissions are offer extreme flexibility in terms of gearing ratios which makes them well suited to taking power from flywheels. The downside to current

CVT transmissions is their low efficiencies that arise as a result of their complex mechanical systems. The low efficiencies in current transmission systems coupled with the high potential for flywheel usage in energy storage systems leave a large area for progress to be made in this subject area.

Switch-Mode PWM CVT Concept

The concept that our MQP team helped to realize with our project is aimed at providing a unique, highly scalable mechanical transmission system which can use the energy within a flywheel extremely efficiently. Research in the Mechanical Energy and Power Systems Lab at WPI on what is officially titled the Switch-Mode Pulse-Width Modulated Continuously Variable Transmission System began with graduate research in 2008 and at the time of this paper, has progressed to the prototyping of the entire system with the end goal of a functioning proof of concept. The Switch Mode PWM CVT concept, outlined in Figure 5 functions as follows:

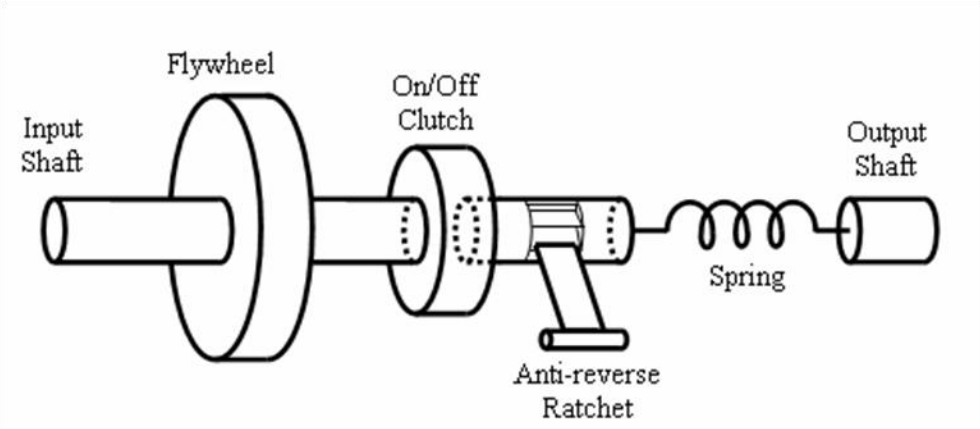

Figure 5: Switch Mode PWM CVT Concept

In the system outlined in Figure 5, energy flows from left to right. The flywheel in the system serves simply as the energy storage medium in the system. Directly coupled to the flywheel is a high speed, low slip clutch which is capable pulse width modulation. An anti-reverse ratchet is connected to the output of the clutch to prevent back driving in the system during energy out mode. In regeneration mode, the ratchet will disengage momentarily to allow energy to transfer back into the flywheel. Connected to the shaft after the ratchet is a complex torsion spring which serves to minimize acceleration and jerk within the shaft. When

functioning properly, this concept functions as a mechanical analogue to the electrical boost-converter circuit shown in Figure 6. By engaging and disengaging the clutch extremely quickly as well as by varying the duty ratio (the percent of time the clutch is engaged over its set period) a pulse-width modulated, virtually continuously variable transmission may be achieved as the amount of energy taken out of the flywheel can be very precisely controlled. The concept is described in greater detail below.

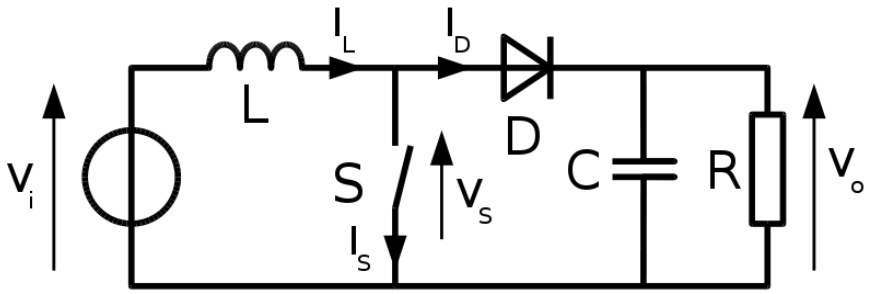

Figure 6: Electrical Boost Converter Circuit

As mentioned previously, the continuously variable transmission concept takes advantage of pulse width modulation to take energy out of a flywheel. A PWM signal is a square waveform which operates at either a high or low value; the ratio of high value to low value can change in order to vary the power flow through the circuit. A sample PWM signal may be seen in Figure 7. Electrical engineers use PWM signals to control the output of a load in the circuit, such as a light bulb. By rapidly varying the duty cycle, or the percentage of time spent at the high value, a light bulb can be made to dim or brighten (Wolff). In reality, the circuit is simply changing the percentage of the time the light is on over the course of a very short (so short the human eye cannot discern the pulses) period.

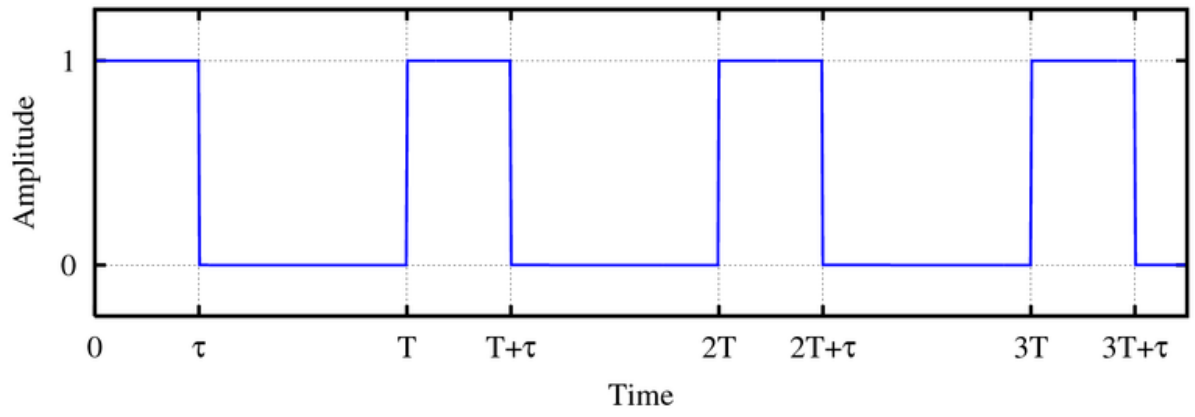

Figure 7: Pulse-Width Modulation Signal (Anonymous, 2010)

In the mechanical equivalent of the boost converter circuit, the clutch is what serves as the high speed switch. By rapidly engaging and disengaging the input shaft, the clutch takes small amounts of energy out of the flywheel and transfers them to the output shaft. As with an electrical circuit, in the energy output, the duty cycle can be varied, allowing the percentage of energy transferred to the output to be easily controlled. Figure 8 shows how the energy is distributed throughout the system. Currently the MEPS lab has developed a high speed, low slip clutch which meets the Note the PWM signal carries through to the output, resulting in nearly infinite spikes in acceleration and jerk in the output of the system.

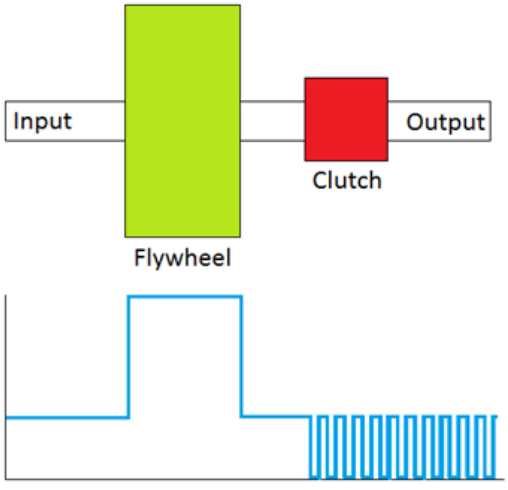

Figure 8: PWM Signal of Switch-Mode CVT

Torsion Spring

One accepted outcome of producing a mechanical PWM signal is that extremely high accelerations and jerks are transferred to the output shaft. Intense accelerations and jerks can rapidly degrade a system by fatiguing the metal. This, in turn, dramatically shortens the lifespan of the system as a whole as the time needed to produce total failure is lessened. To address this issue, an additional stage was added to the Switch-Mode CVT system in the form of a torsion spring/damper which would theoretically minimize these effects. The principle driving the addition is that the torsion spring provides a resistance force, lessening and smoothing out the accelerations in the PWM signal. Ideally, the spring would change the pulses into a continuous, smooth output with minimal energy losses in the system. The brake/ratchet in the system allows for regeneration by allowing energy to be stored in the spring before releasing it into the flywheel. The final system design and the optimal energy response may be seen in Figure 9.

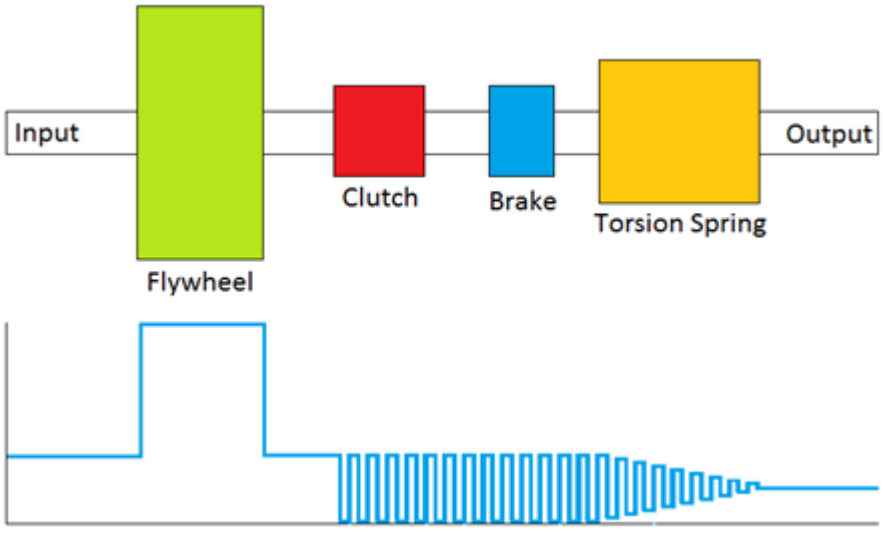

Figure 9: Switch-Mode CVT System and PWM Signal

Previous Research

The design of the Switch-Mode CVT began in 20098 as graduate research conducted by Tyler Forbes. After the concept's potential had been shown on paper, work was transferred to a Major Qualifying Project group of undergraduate students at Worcester Polytechnic Institute (WPI) in 2009. Working with Professor James D. Van de Ven, the group investigated various

clutch, flywheel, and torsion spring designs and developed a scale model as a proof of concept. Some of these original components, such as the test bench and the flywheel, are still in use. The original spring produced by the group was constructed of long, thin, metal sheets which were secured radially between two metal disks. These disks were then used to mount the spring to the system. Figure 10 depicts the original torsion spring developed by the MQP team.

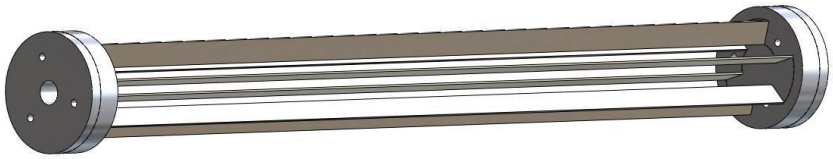

Figure 10: Original Torsion Spring Design (Morocco, Lambusta, DeMalia, & Araujo, 2009)

During the previous group's testing of the spring prototype, the spring bars detached from the prototype causing a catastrophic failure during operation. The failure served to emphasize how important the torsion spring was to the system and made it clear that much more in depth design was necessary before the system would be able to operate properly.

In 2010, the clutch was updated as the result of further research by Jessy Cusack, a graduate student at WPI. With the remainder of the components of the CVT completed, full time devoted work could begin on developing a torsion spring which could meet the strict requirements of the system.

Background Research

Before the group could begin the ideation phase, extensive research was conducted into as many aspects relating to the project as possible. The benefits of this background research were many as the knowledge gained both helped the group understand the task at hand better while also allowing better overall judgments to be made with respect to the design and analysis processes. A summation of the research conducted follows.

Torsion Spring Background

Completing background research for the problem that the group was presented with was a unique undertaking. Before an in depth study was conducted into springs in areas such as

patents and internal stress calculations, the group made a brief investigation into existing systems where torsion springs are used.

There are many applications where torsion springs are used but the most common applications for torsion springs include vehicle suspension systems, garage door lifting devices, and mechanical watch movements. Torsion springs are found in suspension systems for some cars because they offer a cheap, simple alternative to more advanced systems. Torsion springs used in this manner are essentially hollow bars and, while they do exhibit linear spring rates, are extremely large. Torsion springs used in pickup truck suspensions for example, are regularly the length of the entire truck bed. Clearly, the size of the spring disqualifies it from being a viable option moving forward. The types of torsion springs used in watch movements and in garage door openers both exhibit the quality of having a relatively constant spring rate independent of deflection. When springs of this nature are wound, their resistance does not increase until they near their maximum deflection; this is clearly not a suitable characteristic for a spring to have if it is to be put to use in the group's project.

A spring fitting the necessary criteria does not exist at present and as such there was not much applicable research or physical examples for the group to draw from. Basic background research into the theory behind spring forces and such was conducted however so as to give the group a level of understanding appropriate for the task ahead.

Patents

The patent research conducted by the group, though generally unsuccessful, did provide a few notable examples of ideas that the group was able to pull from for the ideation phase of research. The first of these patents was titled "Torsion Spring Type Damper Disc" which consists of two essentially flat cylinders that are attached to each other by springs mounted circumferentially around the interacting faces of the cylinders. The device provides rotational resistance by transferring rotational force into linear spring force (Takeuchi, 1992). The general setup of the spring may be seen in Figure 11. This patent was important to the group's research as it proved the validity of using compression springs in this arrangement.

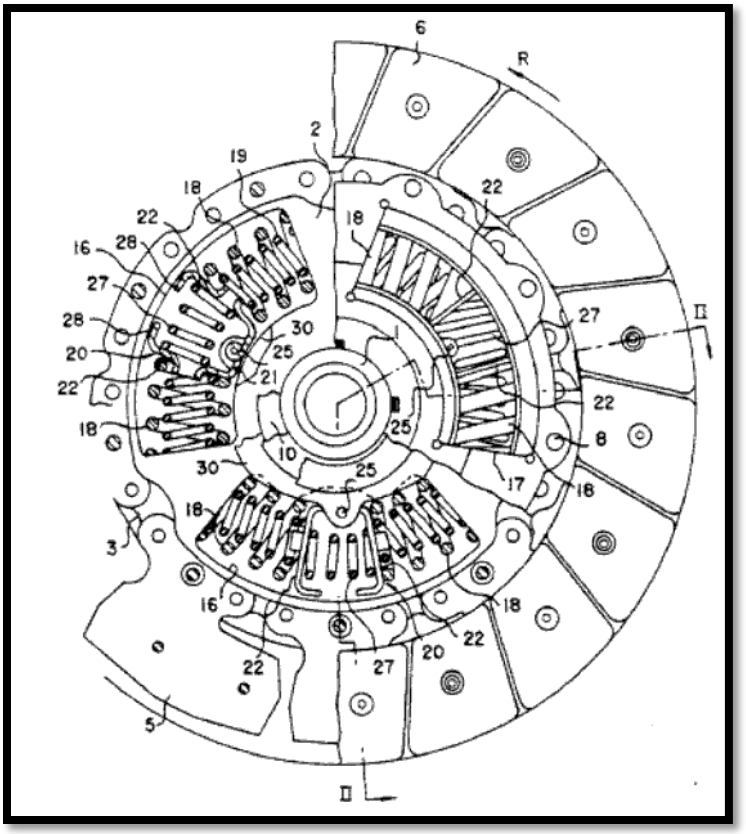

Figure 11: Torsion Spring Type Damper Disc (Takeuchi, 1992)

The second patent that the group drew from extensively presents a novel design for a torsion spring. This patent 'Torsion Spring' filed by Einar Jonsson consists of multiple layers of what are essentially cones of rubber and metal (Jonsson, 1959). A picture of the spring may be seen in Figure 12. This particular torsion spring design is unique in that the possible deflection of the spring may be altered simply by adding or subtracting layers of material. This ability gives the spring design essentially infinite deflection capabilities. In the end, very few patents were found that were helpful to the group's research. This was not entirely unexpected however.

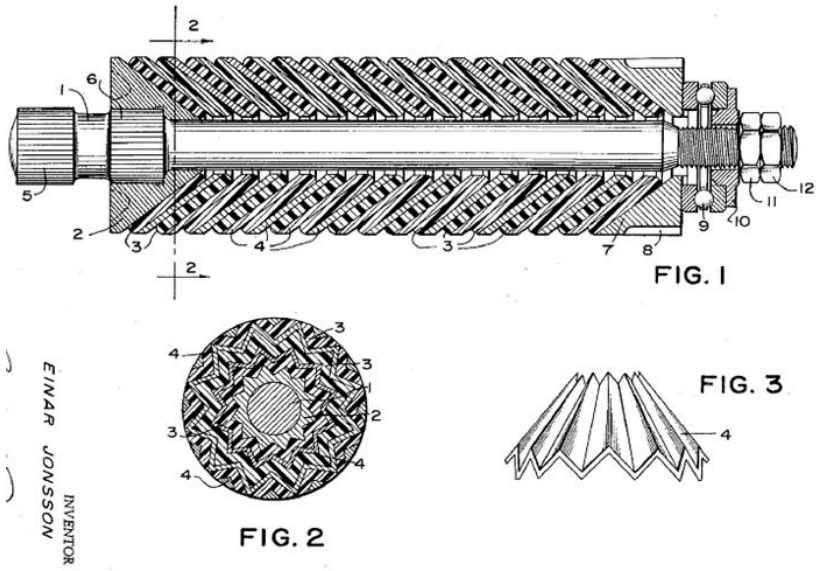

Figure 12: Torsion Spring Design (Jonsson, 1954)

Helical Torsion Springs

Apart from the aforementioned two patents, nothing that directly aided in the group's research was found while conducting a broad patent search. Research was however conducted through other routes and methods. During a simple web search for 'Torsion Springs' the group came across a type of torsion spring called a machined spring. Machined springs are essentially solid hollow cylinders that have had helixes cut out of them in relief. The cuts turn the once-solid bar into a torsion spring with very exacting and precise characteristics. Further, machined torsion springs have helixes with rectangular cross sections which, in certain cases, allow them to have a linear spring rate. Linear spring rates are not found on many helical torsion springs and the fact that machined springs exhibit them was merit for more research. Through a handbook on springs published by the Society of Automotive Engineers detailed information was found on springs with rectangular cross sections. From these sources the group was able to obtain equations that could be used to accurately calculate spring rates, internal stresses, and maximum allowable deformations. These equations were used when considering machined helical springs, and are discussed later in the report. An example of the helical spring calculations may be seen in Figure 13.

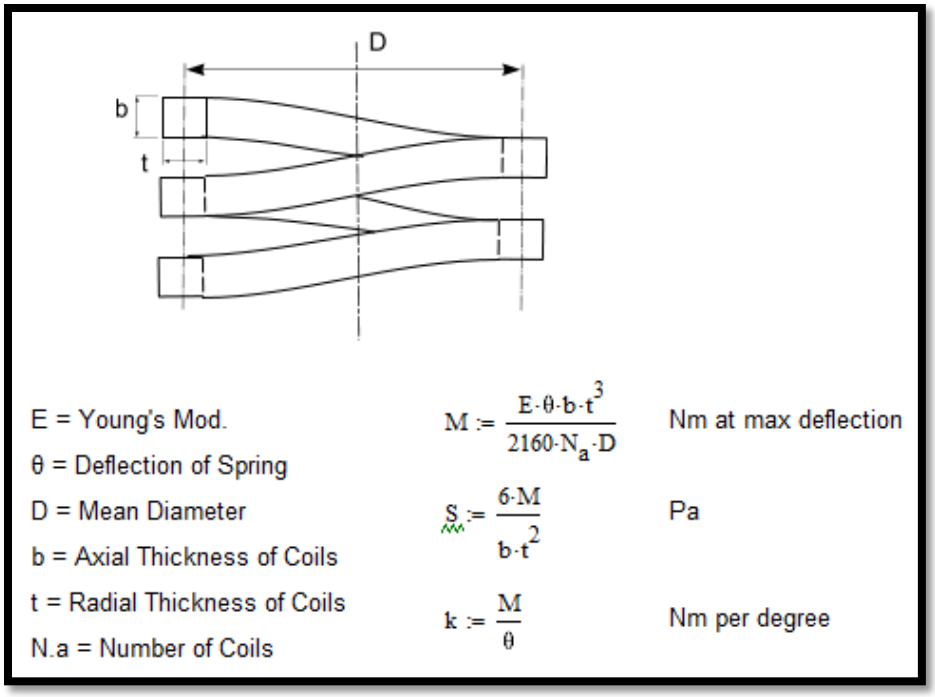

Figure 13: Rectangular Cross Section Spring Calculations (SAE International, 1996)

Through contacts with a company called "Helical Products Inc." further information was gathered about torsion springs. The company, which manufactures machined springs for use in such things as the NASA Mars Rover projects and fin deployment systems for surface-to-air missiles, was able to provide estimates of size, material and manufacturing requirements that the group used in its design evaluations.

Cams

When considering designs of torsion springs which used cams in some way, the group considered many novel concepts. Because cams are not traditionally used in torsion spring applications, the group was presented with a unique challenge. Normally, side loading forces and pressure angle are both minimized during traditional cam design but for the purpose of using an open face cam to transfer torque, these forces were exactly what the group wanted to produce. It was therefore extremely important to understand the rules of cam design so the group could determine which rules could and should be broken. With help from Professor Robert Norton and his book *Cam Design and Manufacturing Handbook* the group was able to

learn key facts which helped in the cam design. One major fact of these deals with pressure angles, or the angle at which force is transferred through the contact point of the followers on the cam. The general rule of thumb for pressure angles is that they should not exceed 35 degrees, but this is not the case for this group's purposes (Norton, Design of Machinery, 2010). In order to transfer the rotational forces accurately, the group decided to raise this pressure angle well over the recommended limit in order to help with torque transfer. Friction and side loading were still major considerations for the group however as they cannot be ignored.

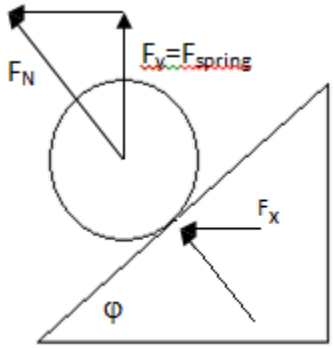

Figure 14: Cam Face Force Diagram

The free body diagram above shows the breakdown of forces and how the linear spring force is converted into torsional force within the system. Through simple trigonometric calculations the force, which defines the torque, can be shown to be:

$$F_x = F_{spring} * \tan\varphi$$

This equation shows that the optimal angle for transfer of force is 45 degrees as that is the angle at which rotational movement and linear movement are equated. If possible however, the 35+ degree pressure angle rule should be followed for efficiency. As seen in the design section, these calculations were very useful in the later creation of the group's cam-based concepts.

After conducting extensive background research, the group understood the problem very well and was able to outline specific objectives and constraints for the project.

Objectives

The goal of this project is to design, build, and test a torsion spring design which exhibits low energy loss, high deflection and low moment of inertia in order to efficiently transfer energy from the flywheel to the drivetrain in the PWM CVT concept. The secondary objective of the group's project is to further the Mechanical Energy & Power Systems Laboratory's development of a fully-functional prototype of the Switch-Mode CVT.

In its design, the device is limited by a number of mechanical and physical factors which are based on results from the previous groups' work as well as Professor Van de Ven's research.

The mechanical requirements of the system are:

- The spring must be able to accommodate up to 70 Nm of torque during use.
- The spring's inertial characteristics must be minimized in order to reduce energy loss.
- The spring must operate under both clockwise and counter-clockwise motion equally well to allow for reverse and regenerative breaking.
- The spring must have nearly infinite life span
    - 10^8 cycles for testing
- The spring must effectively minimize acceleration and jerk at the output.
- The device must have a near-linear spring rate
- Maximum spring length is 18 inches or 46 cm.
- Maximum spring diameter is 12 inches or 30.5 cm.
- Minimum spring deflection of 180° or π radians.
- Must be scalable to work with standard vehicle energy and power requirements.

Design

Initial Designs

After researching successes and failures and doing overall background research into spring design characteristics the group sat down to begin the ideation process. Taking modifications of designs from the past while also coming up with some brand new ideas left the group with eight separate designs. Many of the concepts were extremely unique; some involved magnets as spring replacements and while others transfer rotational torque into linear springs. All of the designs did however show promise which is why the group discussed the pros and cons of each extensively. The eight designs were the magnetic damper, a cam spring, a magnetic series spring, helical spring, wire spring, rotini spring, machined spring, and a torsion piston. Each design is explained below in the order that they were considered.

Magnetic Damper

The first design considered was the magnetic damper system. The basic idea behind the device was to have input and output shafts completely unconnected from one another with a transfer of the rotational movement through magnetic fields. The advantage of this design was the small amount of losses because there are no physical contact points where frictional losses could occur. Further, magnets, as opposed to springs, have a nearly infinite life where as springs exhibit fatigue over time and lose their strength.

The major downfall of the magnetic damper system was the group's limited understanding of magnets and the magnetic fields created by the device. With the limited understanding that the group had three iterations were completed that were all projected to have the same performance characteristics.

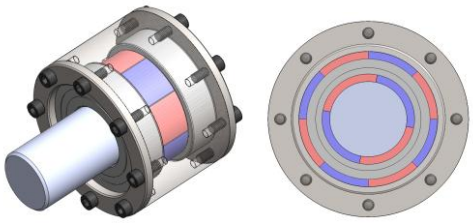

Figure 15: Magnetic Damper Iteration 1

The first iteration has the input shaft inside of the output shaft with magnetic poles arranged radially on the magnets and is shown in the cross section drawing above. This iteration represents how the design was first imagined however due the direction of the magnetic forces the design needed to be reformed.

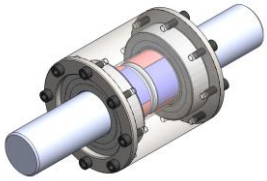

Figure 16: Magnetic Damper Iteration 2

Knowing that magnetic force is felt most perpendicular to the axis of the poles, a second iteration was created that had the input and output collinear to each other and mounted inside a casing to keep them aligned. The problem with this design was the small size of the magnets being used and the small torques they could therefore produce.

Figure 17: Magnetic Damper Iteration 3

In the third iteration the diameter of the magnets being used was increased in order to get the force needed to handle the loading of the system. The downfall to larger magnets is that they become almost like a flywheel and do not possess the low inertial qualities needed for this application.

Cam Separation Spring

The cam separation spring was first designed in the way a standard click pen mechanism works. The pen works using wedges at a certain angle inside of it that translate the linear motion of the button pressing to rotational motion which twists the device that in turn controls how far out the point of the pen is. This spring would follow the same concept and use a radial cam to translate the torque load into a linear compression spring.

Pictured below is the initial cam spring concept where the cylinder and sphere assembly represents the follower and the cam showing the first design of the face. Essentially, the system works because the spring follower system always wants to rest on the lowest part of the cam face. As the input shaft rotates and the follower begins to travel around the cam face the spring begins to compress causing a downward force on the cam face. Because the downward force is being applied to a slope, some of it is turned into a rotational force which is then output to the load end of the shaft. This design pictured is able to rotate approximately 180 degrees and can rotate either direction.

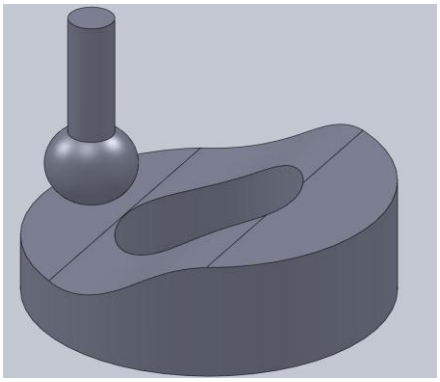

Figure 18: Open face cam design

Further iterations of this cam will be discussed in more detail in the next section of the report.

Magnetic Series Spring

After considering the first magnetic damper design and eventually deciding that is was not feasible, the group came up with the magnetic series spring design. This design stems from the desire to translate linear spring forces (in this case cause by magnets) into rotational torque resistance. The spring design consists of a series of disks with magnets protruding from the

face of the disk in a radial pattern every X degrees (pictured below is 90 degrees). These disks are stacked so that every other disk is offset X degrees leaving the magnets from disks next to each other evenly spaced.

With the magnets assembled in this way it is easy to translate rotation into a linear force. By rotating the input shaft, which is connected to the first disk, the magnets will become unevenly spaced and move toward disk two's magnets. As they move closer the magnets, having polarities arranged so as to repel, will cause a chain reaction all the way down the spring system until it reaches the last disk and output shaft.

The benefits of this design include the standard benefits that come with magnets, no loss due to friction and nearly infinite life. Also because the design is a series of smaller parts it is much easier to scale up and down to meet the requirements outlined in the problem statement. It was for these reasons that the series spring idea was continued into later stages of the design process.

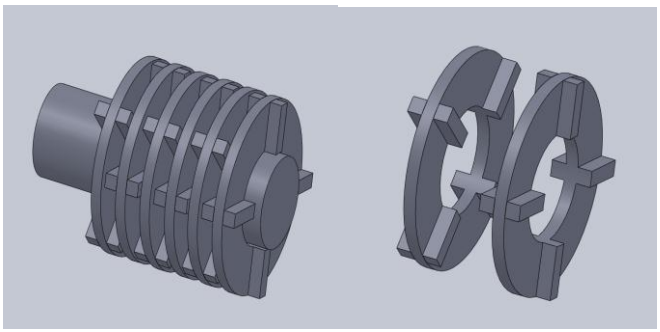

Figure 19: Magnetic Series Spring Design

Helical Spring

The next idea was the closest to traditional helical springs in design with a small modification in packaging. Essentially a number of springs are all combined into one super spring. These springs are arranged in a helical design similar to DNA for packaging purposes. This design focuses on using technology that is already in place, but improving it by making packaging more efficient. Although the design was clever and simple idea the downfall of this design is the limited amount it would actually increase the mechanical properties as it would be

hard to make the spring both strong and light enough to function well while at the same time fitting it into the work envelope outlined in the objectives. Further, linear k rates would be hard to achieve with such a setup.

Wire Spring

While doing research over the summer the group saw the design being considered by a grad student in the MEPS lab and decided to include it in the original design consideration. This design (as the group considered it) consisted of a bar connected to the input shaft. In this shaft are holes, but these holes are not perfectly cylindrical. The holes have the smallest diameter in the center of the bar and it increases as the hole pushes out toward the surface of the bar.

The purpose of these holes is to hold smaller wires/cables with springs attached to the ends. When the bar rotates, the cables begin to wrap around it deflecting their springs. The linear deflections of the springs that are attached to the cables provide the spring rate. The rotational motion would be able to be output if the springs which the cables are attached to are all attached to a separate output shaft which is concentric to the input.

This design has the major benefits of allowing the input shaft of the device to remain extremely small. This gives the device very desirable inertial characteristics. The reasons that the design did not make it past the initial stage of the group's considerations are fairly straightforward; first, the wires going through the center of the assembly will have largely unknown frictional losses because of their winding about the shaft as well as because of internal frictions present in the wires themselves. Second, the group was concerned about the packaging of the device itself and the overall lifespan that it would exhibit. For these reasons the device was discontinued from further consideration.

Rotini Spring

The Rotini Spring design is essentially a solid torsion spring that is shaped like rotini pasta. As another explanation, the spring would look more or less like a twisted ribbon. The idea behind the design is that the odd cross-section of the spirals lend themselves to having more resistance to deflection while at the same time allowing for a higher maximum deflection to be achieved.

The major downfall of this design lay in its unorthodox shape presenting major barriers to force calculation.

Machined Spring

During the group's research, while searching for pictures of torsion springs, a company was found that produces 'machined spring' torsion springs. The company is called Helical Products Co. and they make springs by cutting them in relief out of pieces of solid cylindrical stock. By doing this, the company prevents the spring from being under initial internal loads and also allows the springs to have linear k rates with high deflection angles. The computer model for a spring sized to meet the group's requirements may be seen in Figure 20. Because this design is so similar to classic torsion springs the group predicted that it would be highly efficient while still hopefully having a small package. On the other hand however, the big problem with the spring lay in the precision of the machining required which requires a wire EDM method for production. This design seems to have two major possible issues that the group would have to choose between to consider it for a final design choice; either a large amount of money will be required to machine the part or precision and possibly all of the mechanical properties would be sacrificed if the group attempted to machine a spring at WPI. There is a third downside which is that the spring the group would need for testing essentially maximizes the company's production capabilities which means that the scalability of the design is extremely limited. This is a great design and an extremely good find as a baseline to compare designs to however the costs and overall size are risky.

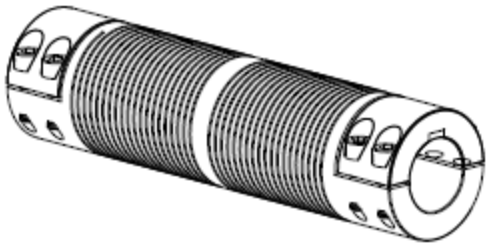

Figure 20: Machined Spring

Torsion Piston

The torsion piston assembly again attempts to convert rotation into linear motion, which can be controlled by a "spring." In this case however the spring is a system with resistance derived from a piston compressing gas. The entire system is made of two springs on each end with the piston system in between the two. When the input shaft turns the first spring would uncoil and begin to lengthen, pushing the piston and compressing the gas. As the gas is compressed it pushes on the piston connected to the output spring. As the piston is pushed it compresses and coils the spring as well and the spring, which tends towards its unloaded equilibrium state, would uncoil and drive the output shaft. The foreseeable downfalls of this design lie mainly in the substantial frictional losses that would be incurred as well as the temperature variations that the gas in the piston would undergo.

Decision Matrix I

With eight designs and three group members, the designs needed to be reevaluated and narrowed down to a number that could be focused on easily. The designs were ranked according to the following ten categories in order of importance: efficiency, lifespan, reliability, inertial qualities, regenerative abilities, cost, size, deflection possible, scalability, and ease of assembly.

Table 1: Decision Matrix Round 1

Characteristics	Weight	Magnetic Damper	Cam Separation	Magnetic Spring	Helical Spring	Wire Spring	Rotini Spring	Machined Spring	Torsion Piston
Efficiency	*14%*	2	3	4	5	3	5	5	3
Lifespan	*13%*	5	3	4	2	2	2	3	3
Reliability	*13%*	5	4	4.5	2	2	3	3	4
Inertial Qualities	*11%*	4	4	3	4	5	2	3	4
Regenerative Abilities	*10%*	4	4	4	4	4	4	4	3
Cost	*9%*	3	3	3	4	2	2	4	3
Size	*8%*	4	5	3	2	5	2	2	4
Deflection Possible	*8%*	5	3	4	4	4	3	4	4

Scalability	*7%*	3	4	3	2	5	2	2	3
Ease of Assembly	*7%*	2	4	3	5	3	5	5	3
	100%	**75%**	**73%**	**73%**	68%	67%	61%	71%	68%

Knowing about each design and looking at the design matrix one can easily see where each design is strong and weak. It is important to note that the three designs the group would research more in depth were not picked because of any single category, but because of their overall performance in the ranking system. The top three designs were the magnetic damper, cam separation spring, and the magnetic series spring with the machined spring coming in a close fourth. However, after looking closely at the magnetic damper and the large amount of unknowns involved the group decided to discontinue consideration of that specific design and decided to pursue the only three designs left: Cam separation spring, magnetic series spring, and the machined spring.

Alpha Prototype Designs

Cam Separation Spring

Although the cam separation spring was selected as one of the final designs it still needed a lot of refining to become feasible. The first issue that needed to be rectified was the unbalanced parts on both the input and output shaft. The follower originally was only on one side; however that could be simply counteracted by mounting a mass on the other side as a counterbalance. The next issue presenting the group was balancing the cam, which, if dynamically unbalanced, would create serious problems when the system is operating at its functioning RPM. The modifications made to fix these problems were to change the cam face so the cam would be balanced and have two high and two low points instead of one of each. The latter change however, cut the possible deflection of the followers on the cam from 180 degrees to 90 degrees, which is below the project's requirement. To counteract this the group looked to putting the cams in series having two of these systems back to back which would make the total possible deflection 180 degrees again.

After realizing that the cams needed to be in series, which would take up valuable space in the overall system the group tried to save space by designing a cam with a symmetrical face on both sides. The resulting design may be seen in Figure 21.

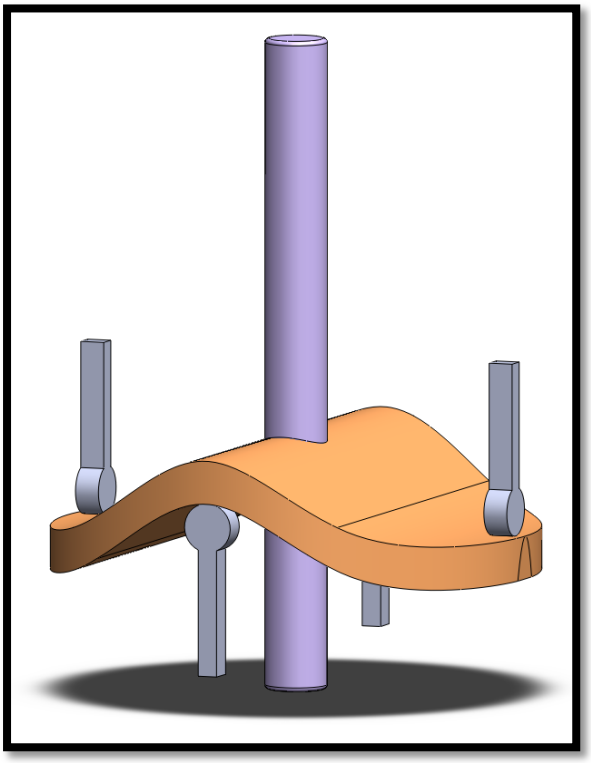

Figure 21: Mirror Cam Assembly

In this case the two followers are attached to both the input and output shaft respectively. The cam rotates independent of the input and output shaft, governed entirely by the follower forces. This assembly works the same way as two cam/spring assemblies in series because when the input shaft rotates the followers will compress the springs and the cam will begin to turn. When the cam turns, it will force the followers on the output shaft to turn as well.

After running some initial calculations with this design it was not possible to get the proper amount of torque necessary without extremely high pressure angles. Therefore, it became necessary to change the placement of the spring to along the shaft and not on each

individual follower. By moving it, a bigger spring can be used and therefore more force and torque can be generated.

Table 2 shows calculations based on spring rate and pressure angle to calculate the torque of the cam system. It is calculated at 75% of the max compression for the reason that ideally the group does not want maximum compression as it would lead to greater losses due to the spring being pushed towards its elastic limit. The table shows that at a pressure angle of 35 degrees (recommended maximum pressure angle) the necessary torque is possible with a 1 in radius system. The next step with this design is to pick the cam face that to be used and then to optimize pressure angle and meet the system requirements. This will be discussed later in the paper.

Table 2: Mirror Spring Rate Calculations

			1 Spring		2 Springs	
			Torque (Nm)		Torque (Nm)	
Radius (cm)	Comp (cm)	Spring Force (kg)	Maximum	75% Comp	Maximum	75% Comp
2.54	3.99	142.8	35.5	26.6	71.0	53.2
3.18	4.99	178.5	55.5	41.6	110.9	83.2
3.81	5.98	214.2	79.9	59.9	159.7	119.8
4.45	6.98	249.9	108.7	81.5	217.4	163.1
5.08	7.98	285.6	142.0	106.5	284.0	213.0
5.72	8.98	321.3	179.7	134.8	359.4	269.5
6.35	9.97	357.0	221.8	166.4	443.7	332.8
	Pressure Angle	45.00	degrees			
	Spring Rate	3760.00	kg/m			

Once the optimal pressure angle was determined, the group used a custom Mathcad program to calculate a seventh degree polynomial cam face curve. The seventh degree polynomial was necessary to control jerk on the cam face. Further, all components of the cam spring were optimized using FEA to minimize their size and mass. Next, any place where friction could occur, either a roller bearing or a sleeve bearing was added to the design. In the end, the group produced the prototype design seen below in Figure 22.

Figure 22: Cam Spring Final Design

Series Spring

The concept for using multiple springs in series originated from two patents. The first patent was for a torsion spring in which small, linear compression springs are wrapped around a shaft as to apply a rotational resistance. When the system is rotated, the springs are compressed linearly which allows the system to exhibit a linear spring rate. Because the springs used circumferentially are simple compression springs, this design allows for inexpensive testing as most of the components can be purchased in bulk. Figure 23 shows the patent.

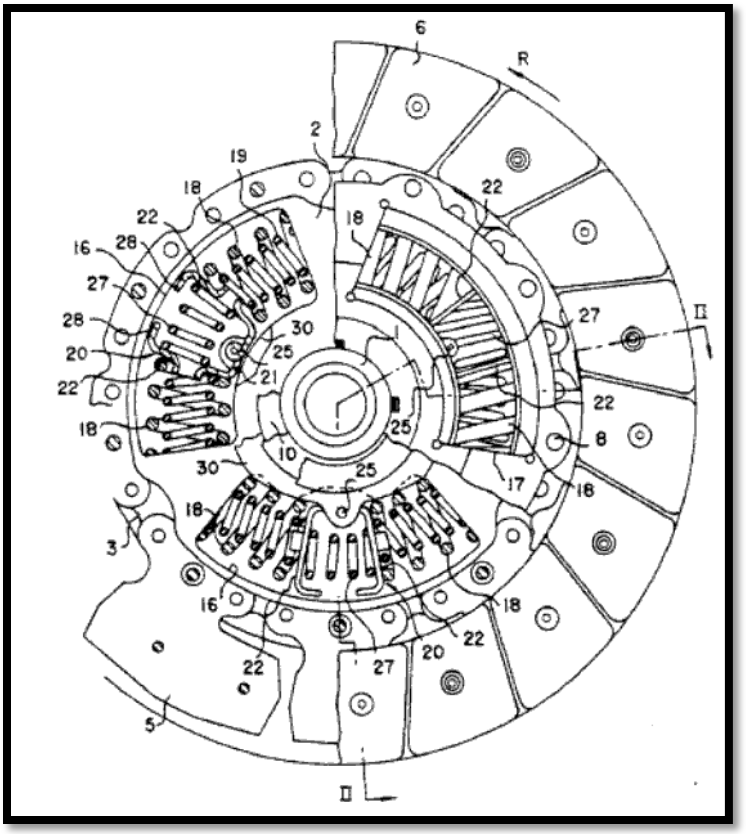

Figure 23: Torsion Spring Type Damper Disc (Takeuchi, 1992)

The second patent which was used in developing this design consists of a series of stacked, jagged cones which alternated between rubber and metal. Although each cone and rubber pair has a very limited maximum spring load, spring rate, and deflection, by placing them in series, the much higher maximum, spring rate, and deflection can be achieved. From this, the concept for using multiple small, linear springs wrapped around the shaft in series was developed. Figure 24 shows an early conceptual design of the system.

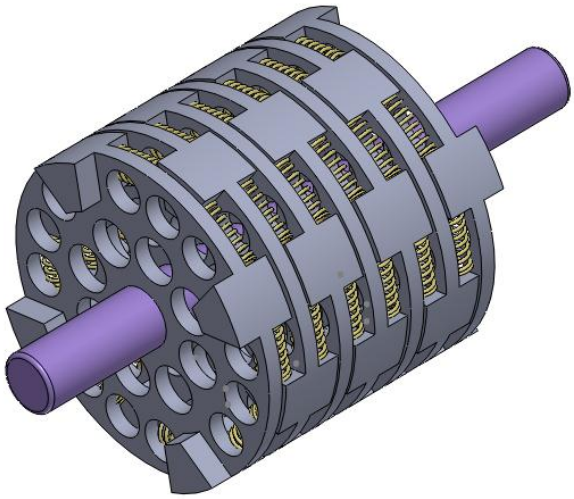

Figure 24: Series Spring Conceptual Design

With this conceptual design complete, equations were developed to describe the system. With these calculations, the diameter of the disc, the number of springs per disc, the spring rate of each spring, and the number of discs were determined. Our final design calls for eight springs per disc, a spring rate above 13 $^{N}/_{mm}$, a 50.8 mm diameter disc, and ten discs. The two major factors in this decision were availability of springs and inertial characteristics.

The next step was to develop a detailed model of the design using these values. This design served mainly as a proof of concept to show that the diameter could be reduced to 50.8 mm. Figure 25 shows the proof of concept model that was developed.

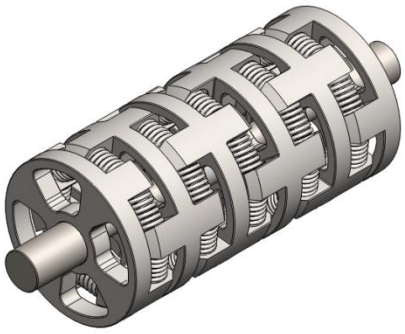

Figure 25: Series Spring Iteration 2

After further discussion, a third iteration was developed. The spring mounts were modified to better support the spring. The spring is placed around the standoff on each mount. The other end of the spring is resting in a corresponding recess on the next mount. This prevents the spring from going into tension, which causes wear in compression springs. Furthermore, the spring mounts are no longer machined from the same piece as the disc. This allows for easier manufacturing, assembly, and repair. Figure 26 shows the input disc with the spring mounts attached.

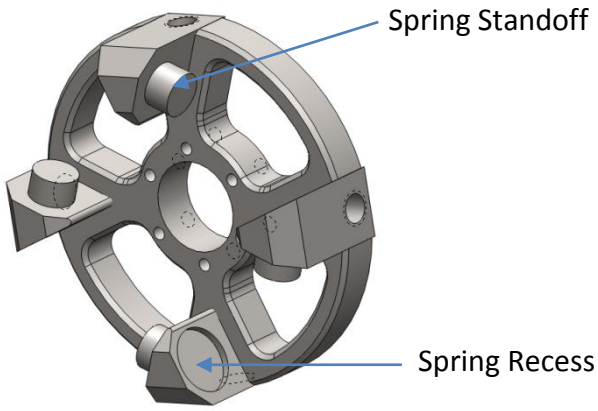

Figure 26: Series Spring Iteration 3

With a completed detailed design, finite element analysis could be performed on the system. A static stress analysis was performed in Ansys Simulation. Analysis was performed on a single disc. For ease of analysis, the center of the disc was chosen as the original with the origin rotating with the disc. This allowed the disc to be simulated as a stationary object, supported in the center, with a torque of 70 Nm at the spring mounts. This corresponds to the maximum force that the selected springs could provide. Two disc designs were tested, with and without the connecting arc between the spring mounts. By eliminating the connecting arc, the inertial qualities of the spring would be reduced dramatically. Figure 27 shows the results of the FEA analysis.

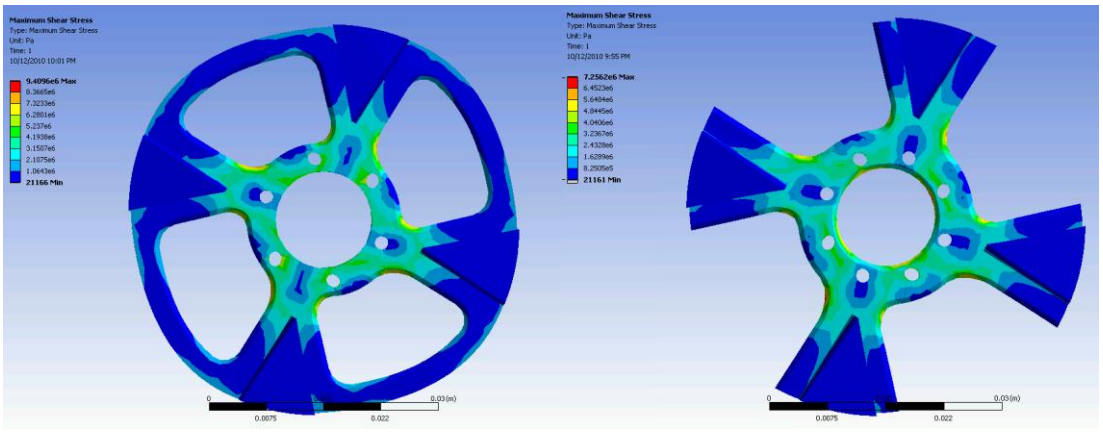

Figure 27: Series Spring FEA Analysis

The FEA analysis clearly shows that the connecting arc has very little effect on the stresses in the system. Furthermore, by increasing the thickness of the supports at the center of the disc, the maximum shear stress in the system was reduced to 7.26 MPa. This is well below the yield strength of carbon steel, which is typically around 200 MPa. With this data, a fourth iteration was developed which will be used for small scale testing. Figure 28 depicts the fourth iteration.

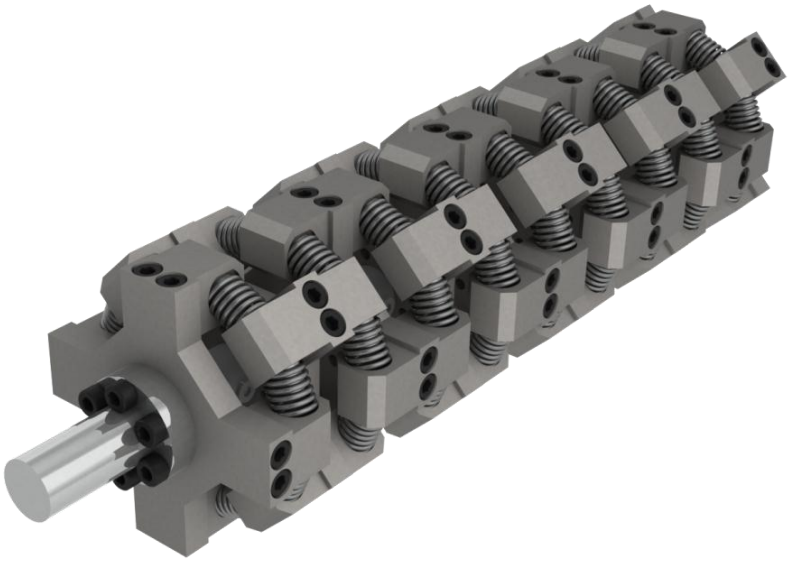

Figure 28: Series Spring Iteration 4

Machined Spring

The machined helical spring was chosen for further consideration because of a few select characteristics. First, the machined spring was the simplest design that the group was considering. As such it had very good theoretical efficiency statistics. Because there are no moving parts in the spring, the only losses that would be seen during the spring's use would stem from internal material damping. Second, the spring, if built from the right materials (superalloys), has the capability of fitting into a relatively small package. Finally, the spring does not suffer from some of the failure possibilities seen in the other two designs, namely the bottoming out possible in the series spring design and the side-load losses seen in the cam design.

In order to go about determining the performance characteristics of the spring itself, the group consulted a firm called "Helical Products Inc." as well as a manual published by the Society of Automotive Engineers to get a better idea of the spring dimensions necessary to fulfill the design requirements. In conversing with a representative from Helical Products Inc. the group was able to get estimated design characteristics for a spring that produced up to 80 NM of torque at 180 degrees of deflection. Further, the group used equations from the SAE manual (seen in Figure 13) to provide a 'secondary opinion' on the size of the spring. In the end, both methods of sizing the spring concluded that a spring with the characteristics seen in Table 3 would be optimal for the desired performance parameters. During spring size optimization calculations, emphasis was put on achieving the necessary deflection and spring rate while at the same time minimizing size and moment of inertia. For example, the overall spring rate is a cubic relation to the radial thickness of the spring coils which means that, where possible, the thickness was increased before the radius, number of coils or axial length of the coils.

Table 3: Helical Torsion Spring Physical Characteristics

Helical Spring Optimal Design	
Length	12in
Outer Dia.	3.5in
Inner Dia.	2.25in
Number of Coils	40
Thickness of Coils	.0787in
Mass of Spring	9.6055lb
Inertia of Spring	4.3158 lb*in²
Material	17-4 PH Steel

In the end, the consideration of this spring design was stopped for two major reasons. First, the machined helix spring has a mass that is very large compared to series spring and mirror cam designs. Second, the size of the spring was given as "right at the manufacturing capabilities" of Helical Products Inc. which means that the spring would be very expensive to machine as well as very tough to scale up without paying an additional premium. For the aforementioned reasons, the helical spring design was eliminated from the considerations indefinitely.

Methodology

Testing System Fabrication

Once the two designs for the torsion spring had been determined, the group set about designing and building a testing rig capable of accommodating both prototypes. The testing rig design was centered about a few necessary facets and constraints. First, the rig needed to be able to contain a flywheel used for energy storage, a clutch, a one-way locking bearing, and an output assembly consisting of either a flywheel or a brake. Second, the assembly needed to be adjustable to hold multiple spring prototypes of differing sizes. Finally, the testing rig needed to be instrumented with multiple sensors for data acquisition. Ideally, the rig design would also incorporate as little internal friction as possible to aid in providing accurate test data.

By adhering to the system requirements and by recycling components and ideas from previous group's designs, the group was able to construct a testing assembly without having to buy very many new parts. The testing assembly may be seen in Figure 29 and consists of a set

of supports which contain, in order from right to left, a flywheel, a clutch, a one-way locking bearing, the spring prototype, and finally support for the resistance source (a disc brake, pulley, or flywheel). The flywheel used was left over from a previous MQP and has dimensions seen below in Table 5. The clutch used was a REELL model EC75. The EC75 is capable of handling 75nm of torque and can pulse at close to 10Hz which makes it very applicable to the type of testing that the group was planning. Further, the clutch engagement time is on the order of thousandths of a second at the loads experienced during testing. Inside of every support block is a rolling element bearing which allows for the efficient transfer of power through the drive shaft. Early in testing, the resistance source came from a simple pulley system which will be described later. After the pulley was used, the resistance source was changed to a disc brake intended for a mountain bike. Finally, the resistance source was changed to a flywheel which was equally sized to the one use to input power. The resistance source was changed to a flywheel because a flywheel is the only load source which truly mimics road load. The pulley and the disc brake assemblies both do not exhibit conservation of momentum and, as such, do not mimic actual road load.

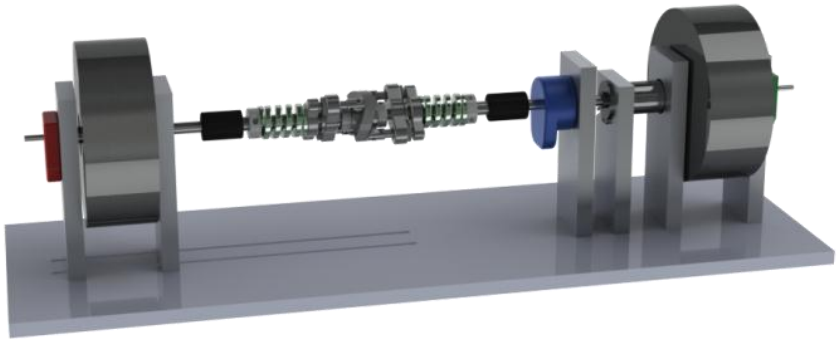

Figure 29 - Testing Assembly with Cam Spring Prototype Installed

Table 4: List of Measurement Devices

Device	Data	Number Used	Model Name
Electronic Clutch	75 Nm Max Torque, 10 Hz Max Freq.	1	EC75 REELL
Rotary Encoder (1/4" bore)	48 to 2048 PPR	2	Amt 102, CUI inc
Rotary Encoder (1/2" bore)	1800 PPR	1	HB6M, US Digital
Hall Effect Sensor		1	Cherry 1013 Series Sensor

Table 5: Flywheel Sizing Table

Variable	Input Flywheel
Outer Radius (in)	4.000
Inner Radius (in)	0.375
Thickness (in)	3.000
Mass (Kg)	19.3
Moment of Inertia (m^2-kg)	.116

In designing the new test stand, there were some improvements that the group was able to make which helped with efficiency and ease overall ease of use during testing. Perhaps the most major of these changes was the fact that the group designed the new testing rig with an output assembly which was able to slide back and forth along the base. The ability of the supports to slide was facilitated by cutting two parallel slots in the test base (See Figure 30) and was extremely beneficial to the group's testing as it meant that little work was required in order to install a spring prototype with different dimensions. Other improvements to the rig, such as boring out the support block which held the clutch in place were also quite beneficial in aiding the overall efficiency of the system.

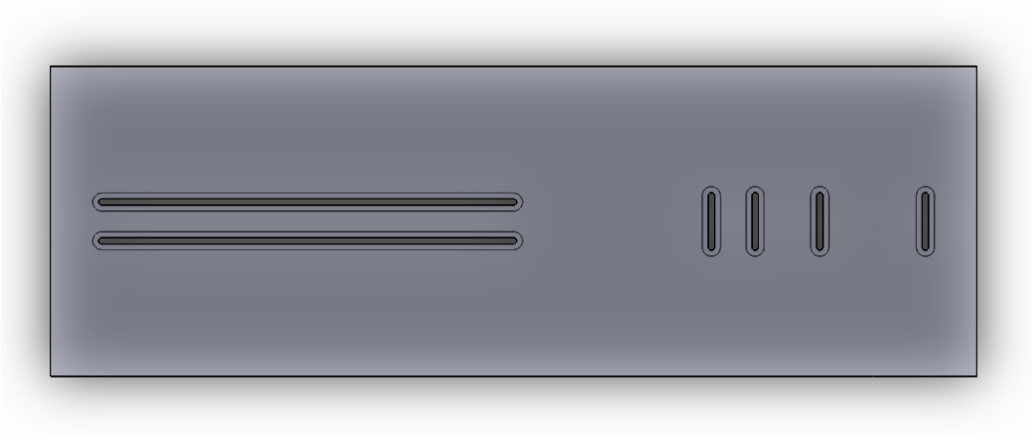

Figure 30: Base of Test Assembly (Bottom Side)

As mentioned before, the efficiency of the trial rig was paramount to the success of the overall testing. In order to minimize internal resistance within the testing assembly, the group was very methodical. First, all moving components in the test stand were given a liberal coating of molybdenum grease to help eliminate friction. Second, each time a new support block was installed in the assembly, its alignment was checked using a pair of calipers to measure the spacing in between the supports on either side in order to ensure the utmost accuracy in the system. If the support was found to be out of parallel by more than a few thousandths of an inch, a plastic mallet was used to tap the system back into alignment. Finally, after each support was installed and aligned, the group rotated the flywheel and shaft within the system to make sure that everything still operated smoothly. This last step was crucial in helping the group determine where key sources of friction were occurring in the system during the early build stages.

Once the testing rig was assembled, the group began to build the safety enclosure with which to encase the rig. The safety enclosure was designed as a large rectangular box and was constructed out of materials strong enough to absorb much of the energy of a catastrophic failure of the rig in the event that one should occur. The group chose half inch plywood to use as the sidewalls and back of the enclosure because of its low cost and relatively high durability. For the top and front side of the box, the group chose to use quarter inch thick Lexan sheeting. Lexan is an extremely durable, optical quality polycarbonate plastic which allows for safe viewing during testing. For additional safety, the vertical joints of the box were secured using

aluminum angle iron, the lid of the assembly was secured by three hasp locks and the whole assembly is attached to the base with screws so that it cannot move during testing. The cad model of the testing rig with the safety enclosure around it may be seen in Figure 31 and Figure 32; actual photos of the safety enclosure may be seen in Figure 31.

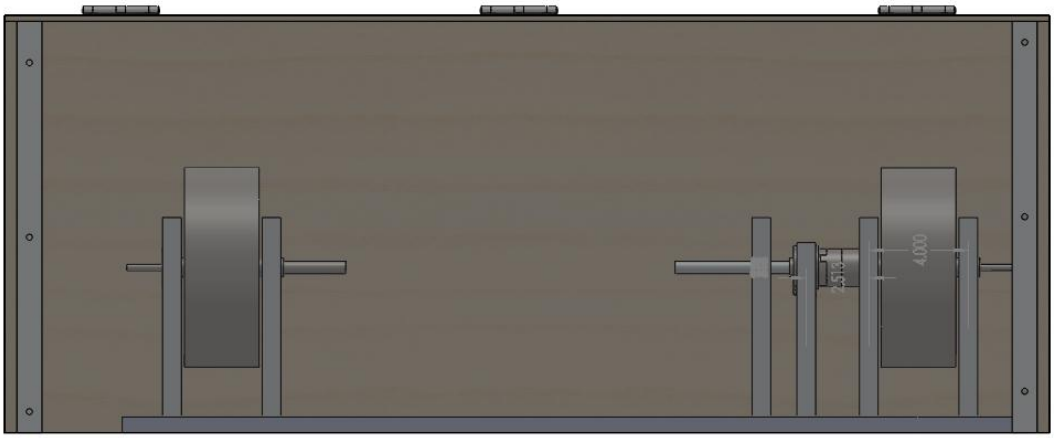

Figure 31: Safety Enclosure - Profile View

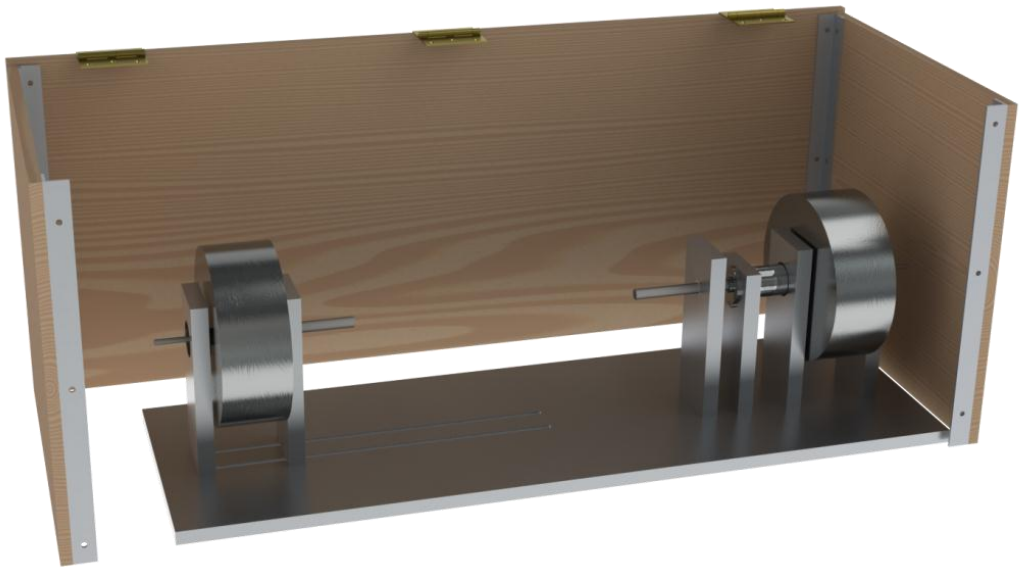

Figure 32: Safety Enclosure with Test Stand

Before testing of the prototypes could begin, sensors needed to be installed on the test stand. In order to measure the RPM of the flywheel, the group installed a Hall Effect sensor and a corresponding magnet. A Hall Effect sensor produces an output voltage when in the presence

of a magnetic field; when that magnetic field is provided by a magnet which moves past the sensor once every rotation of the flywheel, a frequency pulse is. To measure the displacement of different sections of the shaft, the group also affixed three rotary encoders to the testing stand at different points in the system. The first encoder was installed adjacent to the flywheel. The second encoder, placed just after the clutch but before the spring device, was used to record the position of the input shaft of the spring. Finally, the third encoder was mounted to the shaft on the output side of the spring. These four sensors provided all of the information that was necessary to measure the efficiency and performance characteristics of the spring during testing. A table of which sensor was used where may be seen in the appendix along with a wiring diagram for the system as a whole.

Virtual Interface

In order to simplify the testing process, a virtual interface (VI) was created using the LabView® software provided through the MEPS Laboratory. The complete control system consisted of a Dell desktop computer, two data acquisition units (DAQs 6601 and 6220), a transistor switching circuit, and two variable power supplies. The virtual interface allowed the team to easily control system inputs, adjust testing parameters, and monitor and record the resulting data. Figure 33 shows the final block diagram for the VI.

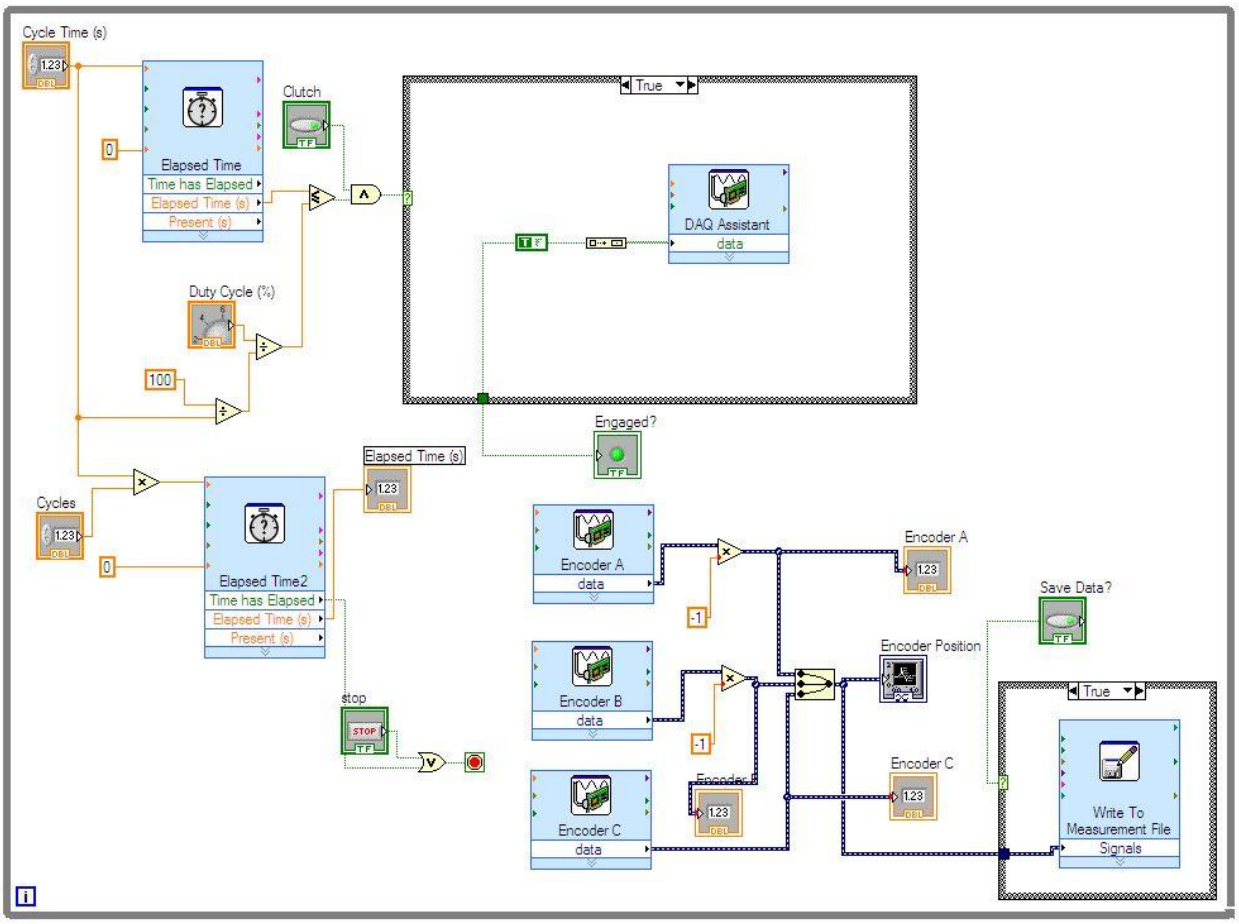

Figure 33: Testing VI Block Diagram

System Control

To simulate the PWM clutch that will be used in the completed transmission, an electromagnetic clutch was used. The clutch, which engages whenever an electric current is supplied to it, was connected to the DAQ through a transistor switching circuit. This was necessary as the clutch has a minimum triggering voltage of 12V while the DAQ has a maximum output of 5V. An N-type TIP120 MOSFET was used. Figure 34 below shows the final circuit design.

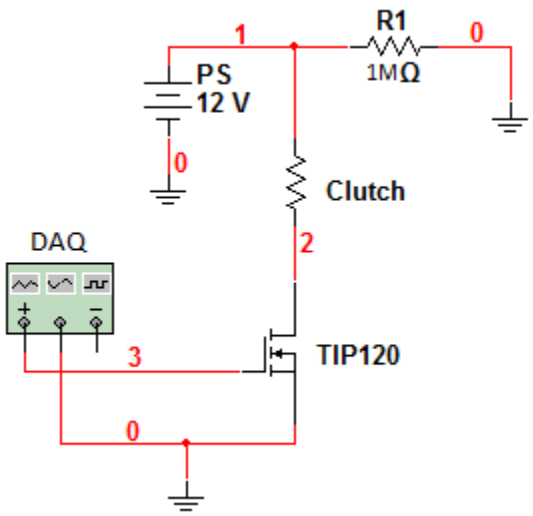

Figure 34: Electromagnetic Clutch Control Circuit

To control the clutch, a PWM signal, sent through the DAQ, is supplied to the gate of the transistor. The PWM signal alternates between a "high" and "low" voltage (5V and 0V respectively). When a high voltage is applied to the gate, the transistor is "on" and the source and drain are connected, allowing current to flow from the power supply, through the clutch, and to ground. When a low voltage is applied, the transistor is "off." To prevent a burnout of the transistor, a voltage divider was added. When the transistor is off, all of the current provided by the power supply passes through the resistor to ground. When the transistor is on, the resistor and transistor act as a voltage divider; due to the substantial difference in resistance between the resistor and the transistor, the vast majority of the current flows to the clutch. This setup allows the VI to control both the frequency and the duty cycle of the clutch. Figure 35 below shows the front panel of the VI.

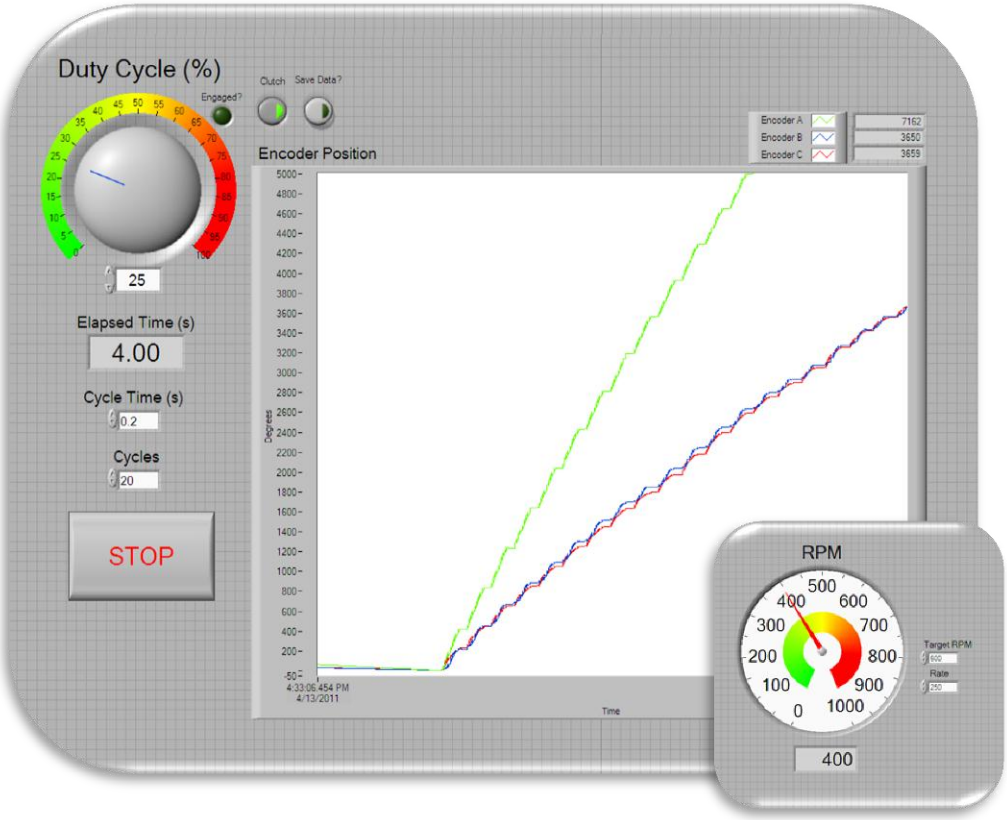

Figure 35: Testing VI Front Panel

Integrating the frequency and duty cycle controls into the front panel of the VI simplified the process of adjusting these parameters between tests. Furthermore, integrating the electromagnetic clutch into the VI allowed for greater automation of the system, dramatically reducing setup time and minimizing the possibility for human error.

Data Collection

Data was collected from the test system through a combination of optical encoders and a Hall-effect sensor. Optical encoders were used to measure radial displacement at various locations in the drive system. The Hall-effect sensor was used to measure the rotational frequency of the input flywheel.

Optical encoders provide an accurate means to measure and compare radial displacement at key locations in the test system. Integrating these into the VI allowed for simple, simultaneous data collection during testing. Encoders were connected to the DAQ USB-6601 and measured by the VI where displacement data from the encoders was plotted in real-

time on the front panel. This allowed the team to easily monitor the system and watch the changes in the system over time.

To measure rpms, the VI calculated the frequency from the pulses sent from the hall effect sensor and used this to determine the RPMs. During development of the test system, it was determined that the addition of the sensor used too much processing power and slowed the computer down. To remedy this, a second VI was created specifically to measure the RPMs. This VI was run only during the setup of each test to measure the initial RPMs of the flywheel.

Testing Procedure

Basic Procedures

The characteristics which were tested in both springs were efficiency and qualitative traits. The qualitative portions were derived from analyzing high speed video of the prototypes during use, which would give the group a good idea of whether or not the concept would work. Efficiency was determined through quantitative analysis of the test data, this process is described below. As outlined previously, the testing rig contained an input flywheel a clutch and an output load (brake or string and mass) which would simulate on a small scale the actual application of the spring. The data needed to calculate the efficiency was only based on energy in vs. energy out. This along with the need for basic observations of the performance quality and the small scale of the systems led to a low scale testing procedure.

Before getting into the details of the test procedure a basic procedure is provided. The procedure simulates what the spring will see in the CVT system. At first the input flywheel is spun up to a designated speed. The speed will vary test to test, but will be picked before the test and measured using the RPM VI. Once the flywheel reaches the desired angular velocity the motor is disengaged and the flywheel is spinning freely at the desired RPMs. After the motor is disengaged the second VI is run. The VI will be preset to the correct duty ratio resulting in the clutch cycling on and off to simulate the load being tested. The VI will also collect the necessary data from the three encoders in order for it to be analyzed later.

Because the testing was low scale compared to what the full size system would be operating at, the RPMs, duty cycles, and loads could also be low. The RPMs were kept under 1000 meaning relatively little energy was transferred through this system. As such, the tests all were completed within 10 seconds of engaging the clutch because the system slowed down quickly. The tests which were run on each spring may be seen below in Table 6.

Table 6: List of Tests Performed

Brake Torque	RPM	Cycle Time	Duty %
.9 Nm	200	0.2	25
.9 Nm	400	0.2	25
.9 Nm	400	0.2	25
.9 Nm	400	0.2	25
.9 Nm	400	0.2	50
.9 Nm	400	0.2	50
.9 Nm	400	0.2	50
.9 Nm	400	0.2	25
.9 Nm	600	0.2	25
.9 Nm	600	0.2	25
.9 Nm	600	0.2	25
.9 Nm	600	0.2	25
.9 Nm	600	0.2	50
.9 Nm	600	0.2	50
.9 Nm	600	0.2	50
.9 Nm	900	0.2	25

Test #	Weight	Distance Lifted	RPM	Cycle T	Duty %
1	1	0.891	60	1	10
2	1	2.875	60	2	10
3	1	7.25	60	2	20
4	1	15.75	120	2	10
5	1	18.25	120	2	10
6			120	2	10
7	0.25		120	1	10
8	0.25	10.25	120	0.5	10
9	0.25		120	0.5	20
10	0.00	0	400	0.2	100
11	0.00	0	400	0.2	10
12	0.00	0	400	0.2	10
13	Stick		400	0.2	25
14	2.5 Nm		400	0.2	25
15	2.5 Nm		600	0.2	25

Series Spring

The first test conducted for the series spring was a natural frequency test. For this test a one pound mass was placed on the weight platform to put the spring under load. Next, the pulley on the output was brought to max deflection. Once it reached max deflection the pulley was released and the oscillations were observed. This procedure was repeated 10 times to gather adequate data. The rest of the tests were done using the basic procedure and the output load described in the section above. The mass of the output system was calibrated using bottles of water because the weight could be varied quickly and easily. The weight was calibrated by adjusting the weight to where the spring would show the load, but it would still have enough deflection left to run an acceptable test.

Cam Spring

Just like in the case of the series spring, the first test run was a natural frequency test. In this case the brake output load was calibrated for the entire test process before the natural frequency test was run. In order to calibrate the brake we adjusted the pressure applied by the brake pads on the rotor using the adjustment screw on the BB-7 braking calipers. The pressure was selected when the output system resisted motion, but it was a small enough torque that the spring still had the force to revert back to its natural resting position. Once the brake was calibrated the natural frequency test was performed in a similar manner, by deflecting the spring to near max deflection and observing any oscillations that occurred.

Results

Round 1

The first round of testing was done in order to narrow make a decision on the last two designs, the cam spring and the series spring. This testing looked for qualitative characteristics such as the series spring bottoming out or the cam spring overdriving, but also looked at quantitative data such as efficiency of both systems. This section is broken up into the qualitative and quantitative results and the final decision matrix. In the final decision matrix the better of the two springs was chosen to be built and tested at full scale.

Qualitative Results

Series Spring

During the design process of the series spring the biggest issue identified by the group involved determining if a large enough deflection could be obtained through this design. This problem was solved by adding more discs until the desired deflection could be achieved. Once it became clear that the spring design would need a multitude of discs, another problem arose. The group became concerned that the initial springs in the assembly would compress too quickly allowing the discs to collide into each other which would lead to early failure of the system. In running the first round of testing the group watched very closely to make sure this didn't occur. Unfortunately In most tests the initial pulse of the clutch was enough for the series spring to bottom out and cause the discs to collide with one another. The bottoming out behavior is directly related to fact that the effective inertia on either side of each disc is different which means that a rethinking of the design would be necessary if it were to be taken to the second round.

The other qualitative test is a test of the concept itself investigates whether the spring demonstrates the appropriate performance qualities. This data was accrued through the analysis of the graphs compiled in matlab, as well as through high speed video analysis. In the series spring very good compliance qualities were demonstrated. Through the high speed

camera the group observed the input with a very jerky angular motion while the output had a nearly constant angular velocity motion.

Cam Spring

The possible problems that the group expected to arise from the cam spring were asymmetrical motion of the followers and the possibility of the followers jumping over the cam. The cam was designed to have two identical faces on each side and corresponding followers. Because the motion of the output followers relied on both the motion of the input followers and the cam the group was not completely positive that the input followers and output followers would mirror each other's movements and therefore unevenly split the load. During both slow speed and high speed analysis, symmetric follower travel was exhibited which validated the concept significantly.

The output system for the testing rig of the cam spring was designed to be a constant torque bike brake. What actually occurred was a varying torque output without inertia. At different angular displacements the torque would increase and decrease based on the transition from static to dynamic friction. This caused jerky motion in the cam spring and without inertia every pulse was similar to starting from a stop. This led to issues such as the cam spring being under load and the followers starting a pulse already halfway up the cam face. At low speeds the cam would take two input pulses in order to get one output pulse. The group coined the term 'double pulse' for this effect. With higher speeds the double pulse effect caused the followers to overrun the cam and lose 180 degrees of input deflection. This problem arose due to the fact that the Lexan supports for the spring would flex too much under load. In the full scale design, there is a physical stopping point that prevents the followers from going past 180 degrees of deflection.

Quantitative Results

Data collected from the optical encoders during testing was used to compare the efficiency of the two designs. Angular displacement, velocity, and acceleration plots were calculated for each test from this data. From this, the efficiency was determined while providing visual

representation of the kinematics of each design. MatLab® was used to simplify the calculations and to generate the resulting plots. The base code was provided by the group's advisor, Prof. James D. Van de Ven, and then modified to accommodate the three data sets recorded per test and to calculate the efficiency.

First, the angular velocity and acceleration curves were calculated, filtered, and plotted from the angular displacement data. First, the initial data sets where filtered to check for and remove outliers. The angular velocity and acceleration were then calculated using a derivative function on a point-by-point basis. The following equations were used.

$$\omega_n = \frac{d\theta_n}{dt} \cong \frac{\theta_n - \theta_{n+1}}{\Delta t}$$

$$\alpha_n = \frac{dv_n}{dt} \cong \frac{v_n - v_{n+1}}{\Delta t}$$

The equations describe the angular velocity and acceleration at each point using a simple slope equation. Although this provides only a localized estimation of the actual derivatives, the small value (0.015625 seconds) of Δt in the denominator results in a good approximation of the actual curve. These curves were plotted for each test. Figure 36 below provides example plots from a test of the Cam Spring. Figure 37 below provides example plots from a test of the Series Spring. The final plots for Round 1 can be seen in Appendix B – Round 2 Plots.

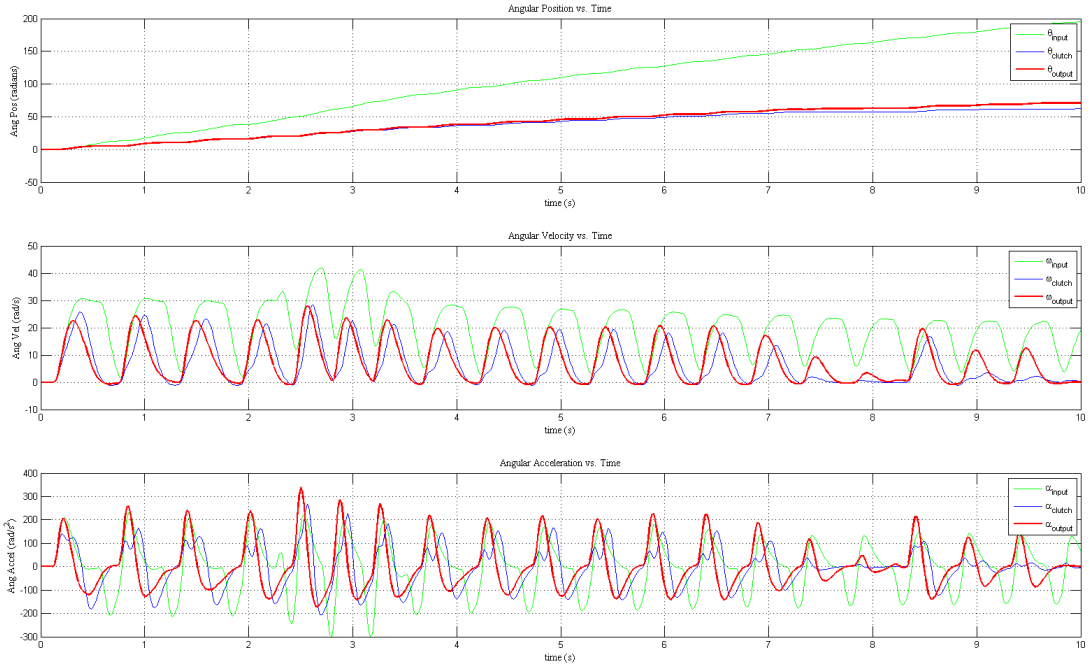

Figure 36: Example Angular Displacement, Velocity, and Acceleration Curves (Cam Spring)

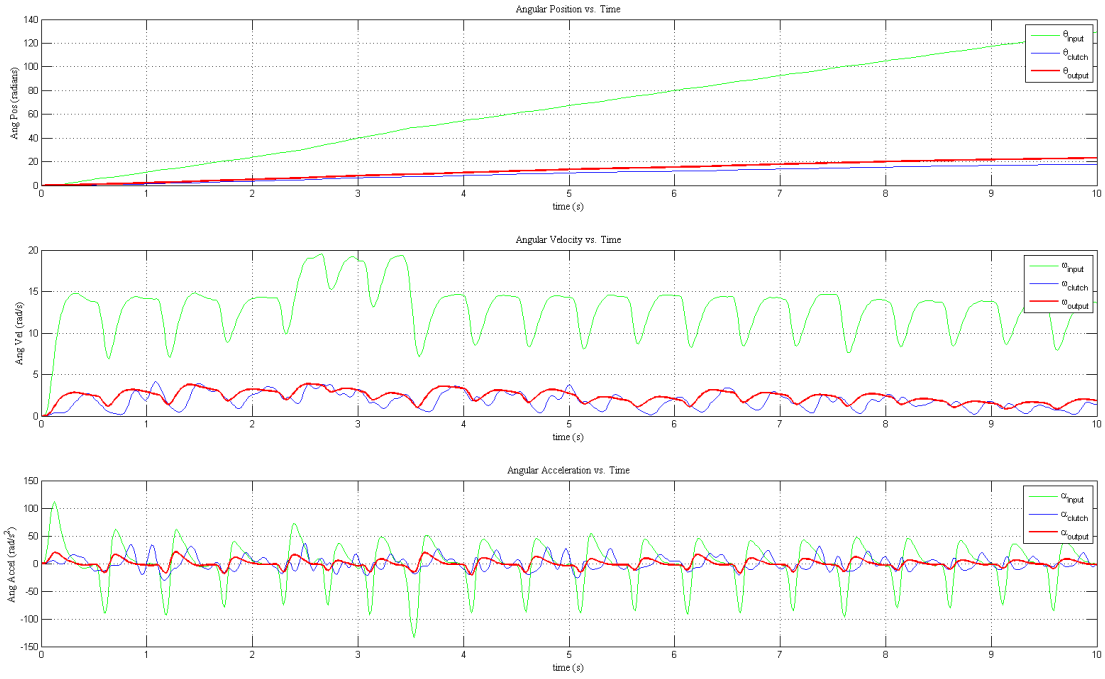

Figure 37: Example Angular Displacement, Velocity, and Acceleration Curves (Series Spring)

Next, efficiencies for each system were calculated. First, linear regression analyses of the angular velocities were made. Using this, the instantaneous kinetic energies of the input, clutch, and output were calculated. Using the same equations used to describe the angular velocity and acceleration, the change in kinetic energy over time was calculated. Finally, the efficiency of each test was calculated using the following equation where the energy output by the spring was divided by the energy put in to the spring.

$$eff = \left| \frac{dKE_{out}/dt}{dKE_{in}/dt} \right| * 100\%$$

The overall efficiency for each design was determined by averaging the resulting efficiency of each test.

In the series spring, the average efficiency of the prototype was found to be %69. The average efficiency of the cam spring was found to be 62%. Both prototypes were less efficient at low speeds and gained efficiency with higher rpms and duty cycles. The individual results of each test may be graphically seen in the Appendix. Raw data of each test may be found on the group's sharepoint page.

Round 2

After selecting the Cam Spring as the final design, production began on the full-scale, final spring. Based upon the performance of the Cam Spring during initial testing, no revisions of the cam or any other aspect of the device were necessary. To reduce manufacturing time, especially for the cam, the final parts were outsourced to a local machine shop where they were machined from AISI 304 Stainless Steel. Upon receiving the completed parts, the final spring was assembled and tested.

Testing took place at 400 and 600 RPMs as well as at various duty cycles. Although the initial methodology called for final testing at 1000 RPMs, problems occurred during testing that could not be overcome. Specifically, the axial thrust resulting from the compression of the linear springs caused binding in the system, despite the addition of the thrust cross-beams. Furthermore, the additional torque applied by the system sheared a pin in the input shaft which locates its rotational position to that of the clutch. Replacement of the pin revealed that the resulting torque for this round of testing would shear the pin within 1-2 tests, making data collection difficult and unreliable. However, data sets that were collected showed that the final system performed as predicted by testing during Round 1.

Qualitative Results

As with the first round of testing, qualitative testing was performed using a high speed camera, taken at 260 FPS. The resulting video shows the Cam Spring functioning as expected; with the spring smoothing the output as well as the Series Spring did during Round 1 testing. This shows that the jerky output exhibited by the Cam Spring during Round 1 testing was primarily due to the output disc brake and not the design itself.

Quantitative Results

As with the first round of testing, quantitative analysis of the system was performed by measuring the angular displacement, velocity, and acceleration. No aspects of data collection were changed. The resulting encoder data was analyzed using MatLab®. The resulting angular displacement, velocity, and acceleration plots (Appendix B – Round 2 Plots) show that the

system performs as desired. Furthermore, by comparing the Round 1 and Round 2 results for the Cam Spring (Figure 38), it can be observed that the addition of mass, and thus inertia, to the system (changing from ABS plastic to 304 SS) results in a smoother angular velocity and acceleration, which significantly reduces jerk in the system. This can also be partially attributed to changing the output to a flywheel. By smoothing the output, fatigue is further minimized in the output shaft.

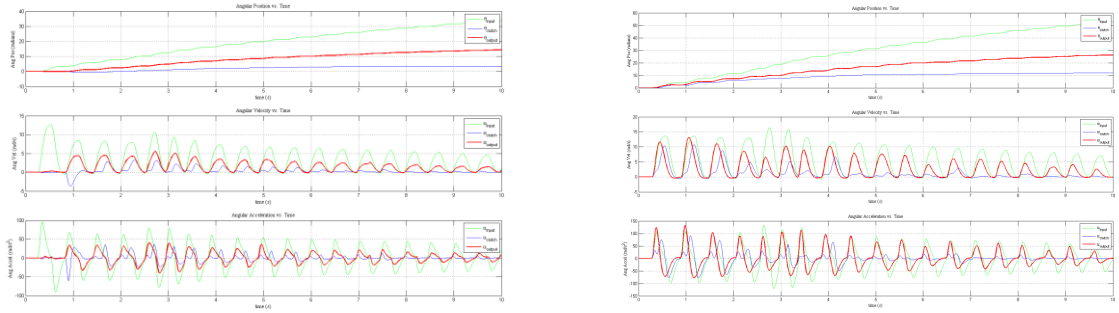

Figure 38: Round 1 (left) and Round 2 (right) Results (600 RPMs and 50% Duty Cycle)

Conclusions and Recommendations

The purpose of the project was to complete the table top model of the CVT system by implementing a torsion spring coupled with the clutch. Three tasks were necessary to accomplish this. First, develop a torsion spring which meets the physical and mechanical requirements of the system. Second, manufacture a full-scale, working prototype. Finally, test the design in a simulated, complete system. The first task was completed by developing, mathematically analyzing using finite element analysis and dynamic calculations as needed, and then narrowing down 14 initial designs. Each of these designs, including the two chosen for prototyping and initial testing, met the physical specifications for size, inertial qualities, and deflection capabilities. From these, two designs were chosen for baseline testing. Adding this step resulted in a greater time requirement. Additionally, the VI took much longer to implement than originally planned.

Initially, the group hoped to facilitate development of the testing assembly by recycling components used by previous groups. However, this resulted in unforeseen setbacks. While the system was well suited for testing during Round 1, which was scaled down to accommodate the materials used, complications occurred during final testing. Specifically, the testing assembly proved unable to withstand the axial thrust loads applied by the final spring. The system output also proved problematic. Using a small flywheel for the series spring worked well. However, using a bicycle disc brake for the cam spring negatively affected the output of the spring as the disc brake could not provide a constant resistive torque nor simulate an inertial load. As such, a disc brake alone should not be used in future testing unless some form of inertia load is also used. This will help better model the output of the CVT system.

Another setback, of the project was the time necessary to machine parts. Despite the use of rapid prototyping during Round 1 testing, development of the initial Cam Spring and Series Spring took far longer than anticipated. This was due to the time required to machine non-rapid prototyped components, such as the shafts. To alleviate this during development of the final design, the final parts were outsourced. However, once the cam spring was selected as the final device, too much time was spent locating a machine shop to do the work. The parts

should have been lined up for either design and as soon as a design was selected the machine shop should have been notified.

These setbacks did not allow for much time to conduct final testing. Furthermore, failure of the testing assembly, as mentioned above, proved a setback. Although the testing assembly developed by the previous Switch-Mode CVT MQP team was theoretically designed to handle 70Nm, the torques generated proved too much for the shaft/clutch alignment pin, resulting in a system failure. This failure lead to an end to final testing due to the time it would take to redesign and remanufacture the testing assembly. Although only limited testing could be performed on the final design, the combination of both small-scale and full-scale testing of the Cam Spring shows that the design functions as intended and meets all of the objectives set.

Although the final Cam Spring prototype (seen in Figure 39) functioned as desired, some future recommendations can be made. A major oversight was the large axial thrust exerted by the Cam Spring under load. This load results in binding in the system support blocks. Modifying the testing assembly proved to not be enough. For future iterations of the spring, this needs to be accounted for in the design. One option proposed by the group is the addition of an encapsulating cage which would be located around the spring. In this way, the thrust then becomes internal to the spring and is not applied to the testing assembly.

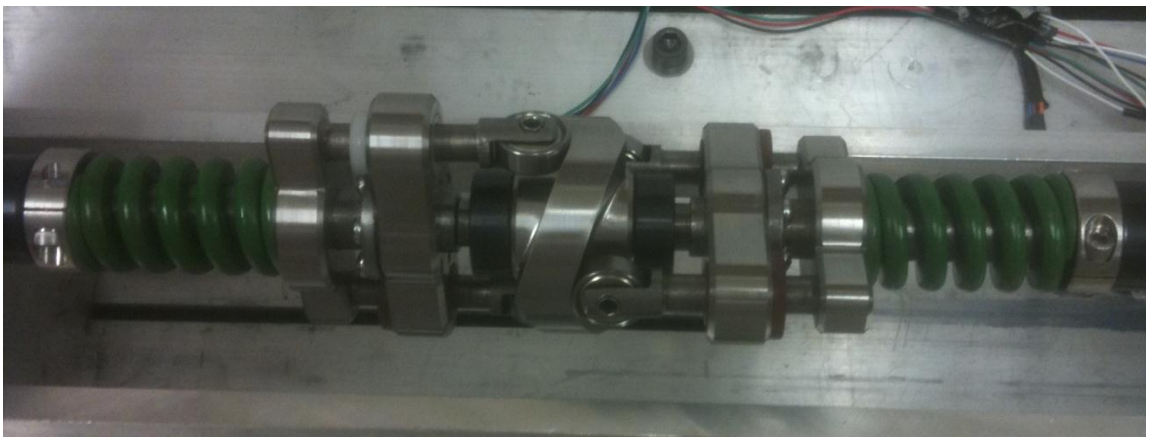

Figure 39: Full Scale Cam Spring Prototype

Overall the project experienced great success in designing and building a torsion spring that could complete the CVT system. The final design is able to smooth the output of the clutch

as desired while still remaining well within the physical requirements of the system. Future work will involve complete integration of the Cam Spring into the full CVT system, including the existing clutch prototype.

References

Anonymous. (2010, September 18). *Duty Cycle*. Retrieved October 12, 2010, from Wikipedia: http://en.wikipedia.org/wiki/Duty_cycle

Baseley et. al., S. (2007). *Power Density versus Energy Density of Various Technologies.* SAE International.

Birch, S. (2010). *Audi takes CVT from 15th century to 21st century*. Retrieved October 12, 2010, from SAE International: http://www.sae.org/automag/techbriefs_01-00/03.htm

Duffy, S. (n.d.). *Hybrid Car Sales Figures*. Retrieved October 12, 2010, from Hybrid Car.

Harris, W. (n.d.). *How CVTs Work*. Retrieved October 12, 2010, from How Stuff Works: http://auto.howstuffworks.com/cvt.htm

Hebner, R., Beno, J., Walls, A., & University of Texas, A. (2002). Flywheel Batteries Come Around Again. *Spectrum, IEEE*, 46-51.

Jonsson, E. (1954). *Patent No. 2,873,110.* United States.

Lawrence Livermore National Laboratories, US DOE. (August 2010). *Estimated Energy Use in 2009: ~94.6 Quads.* Livermore, CA.

Morocco, A. J., Lambusta, C. M., DeMalia, M. A., & Araujo, J. M. (2009). *Switch-Mode Continuously Variable Transmission.* Worcester, MA: Worcester Polytechnic Institute.

Nashawi, I. S. (2010). Forecasting World Crude Oil Production Using Multicyclic Hubbert Model. *Energy & Fuels*, 1788-1800.

Norton, R. L. (2009). *Cam Design and Manufacturing Handbook.* Industrial Press, Inc.

Norton, R. L. (2010). *Design of Machinery.* Prentice Hall.

SAE International. (1996). *SAE Manual on Design and Application of Helical and Spiral Springs.* Warrendale, PA: SAE International.

Takeuchi, H. (1992). *Patent No. 5,163,875.* United States.

Williams, J. L. (2007). *Oil Price History and Analysis*. Retrieved October 12, 2010, from WTRG Economics: http://www.wtrg.com/prices.htm

Wolff, C. (n.d.). *Peak and Average Power*. Retrieved October 12, 2010, from Radar Tutorial.eu: http://www.radartutorial.eu/18.explanations/ex28.en.html

Appendix

Appendix A – Round 1 Plots

The following section contains the angular displacement, velocity, and acceleration graphs that were generated for each test performed on the Cam Spring and Series Spring during Round 1 testing. For an explanation of how these plots were derived, see Round 1 - Quantitative Results.

Cam Spring

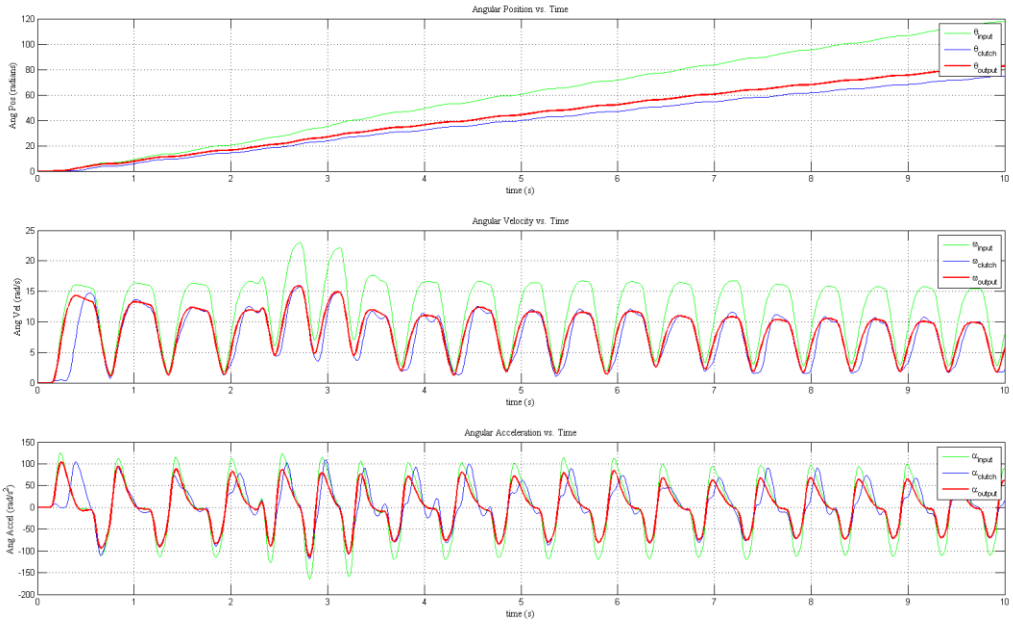

Figure 40: Cam Spring Data Set 1.1

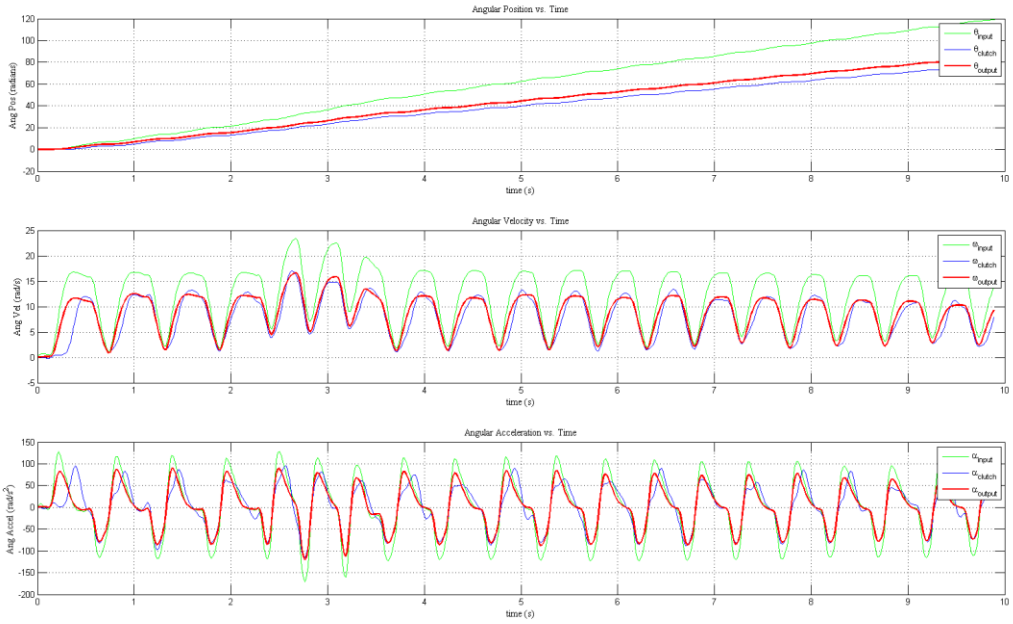

Figure 41: Cam Spring Data Set 1.2

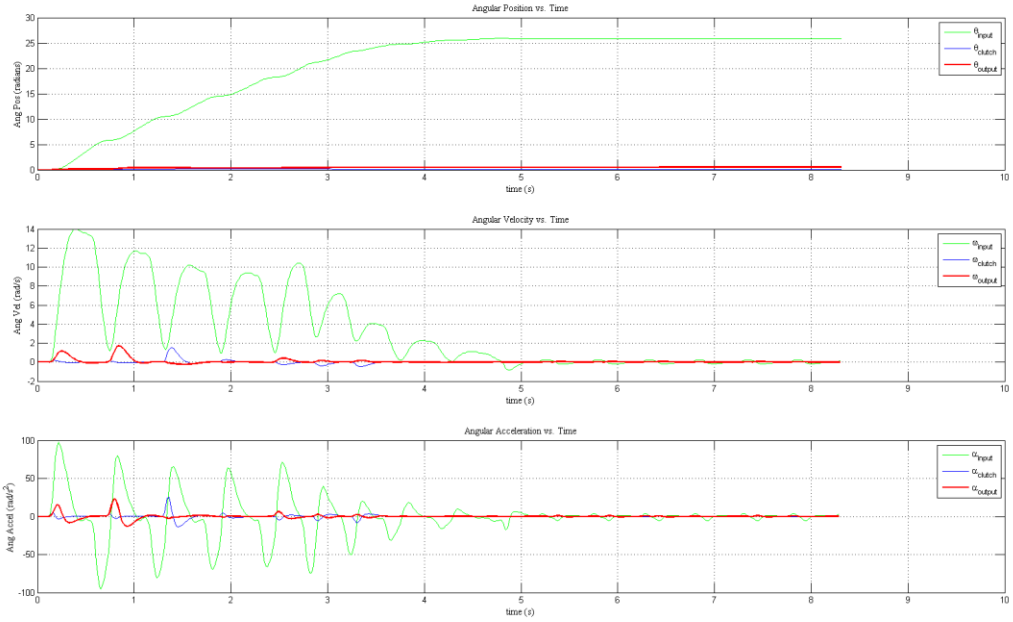

Figure 42: Cam Spring Data Set 1.3

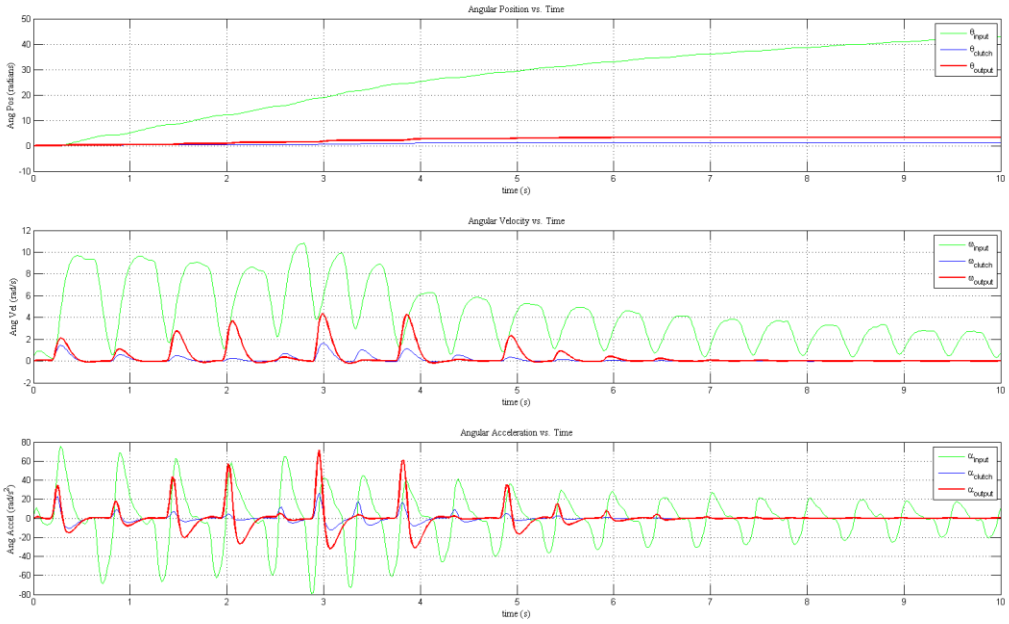

Figure 43: Cam Spring Data Set 1.4

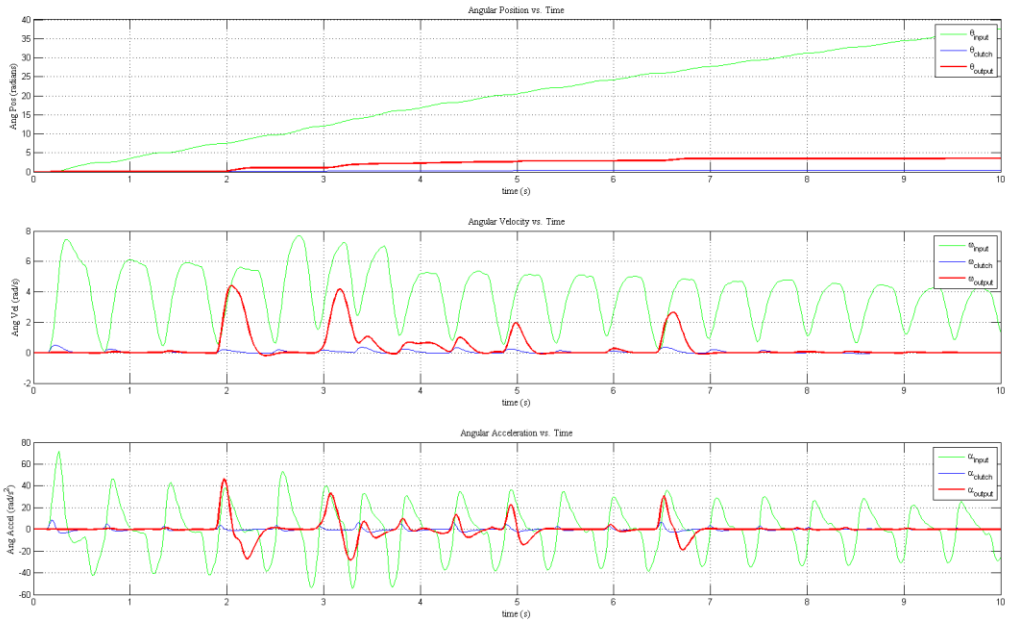

Figure 44: Cam Spring Data Set 1.5

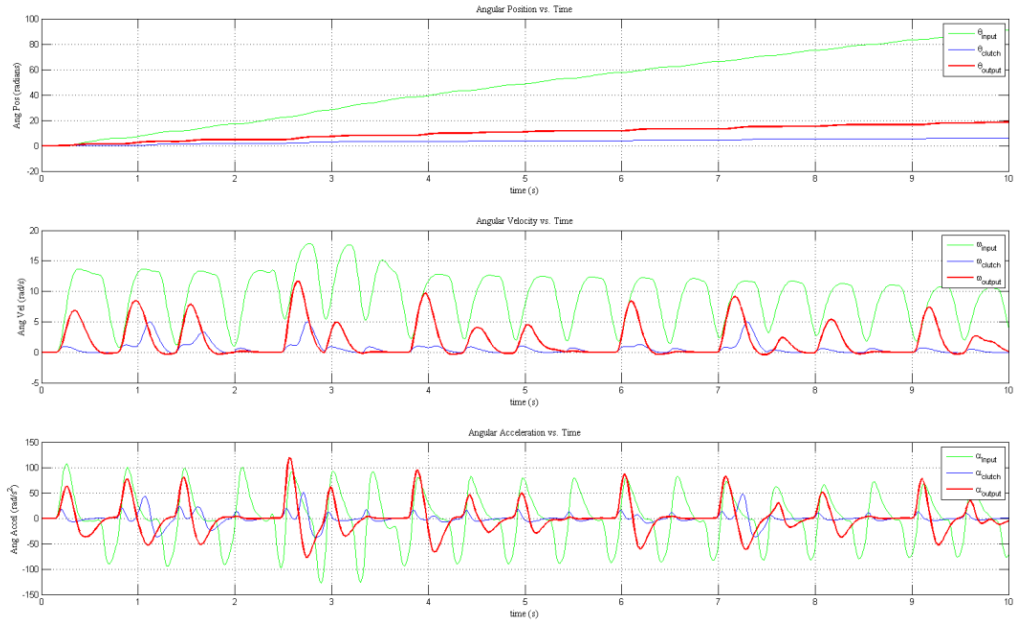

Figure 45: Cam Spring Data Set 1.6

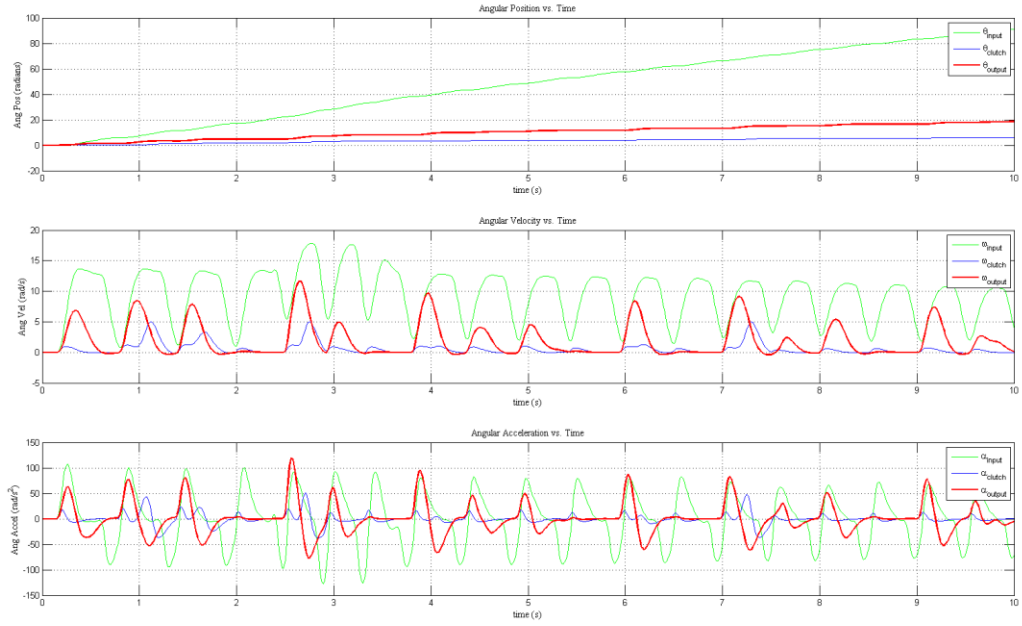

Figure 46: Cam Spring Data Set 1.7

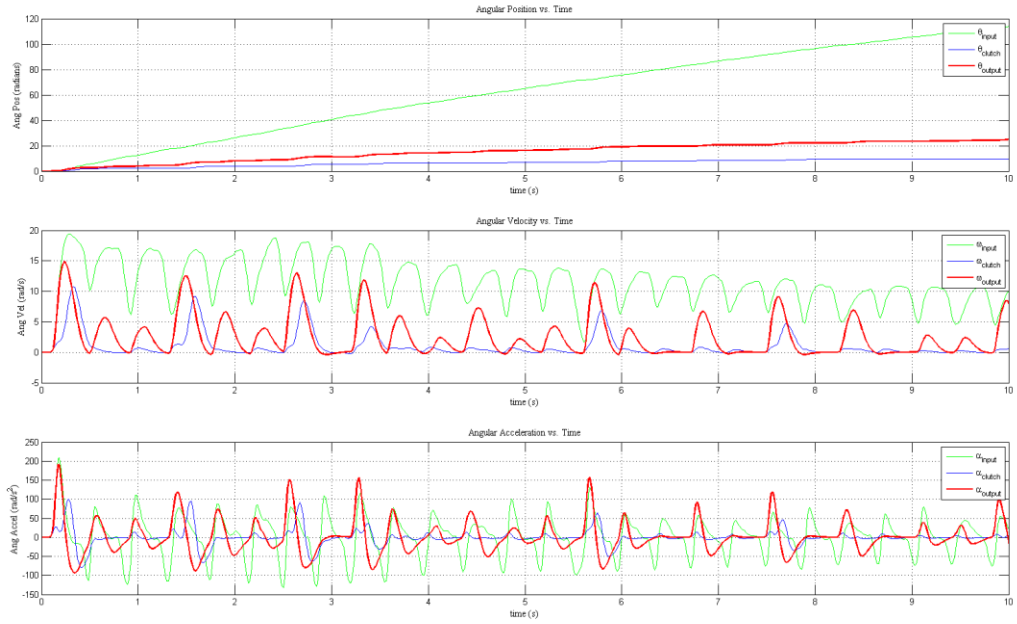

Figure 47: Cam Spring Data Set 1.8

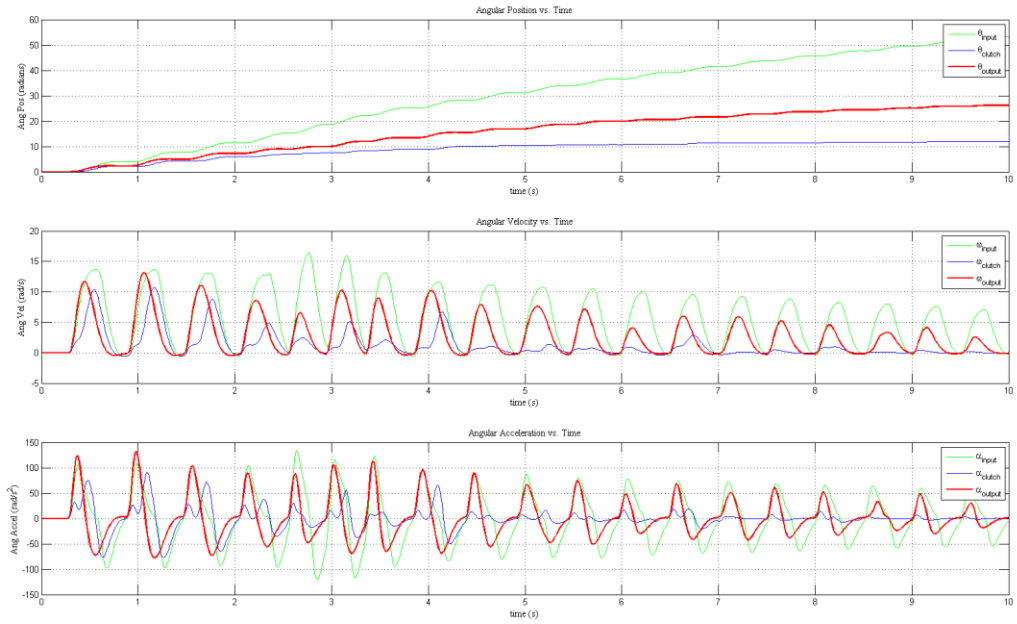

Figure 48: Cam Spring Data Set 1.9

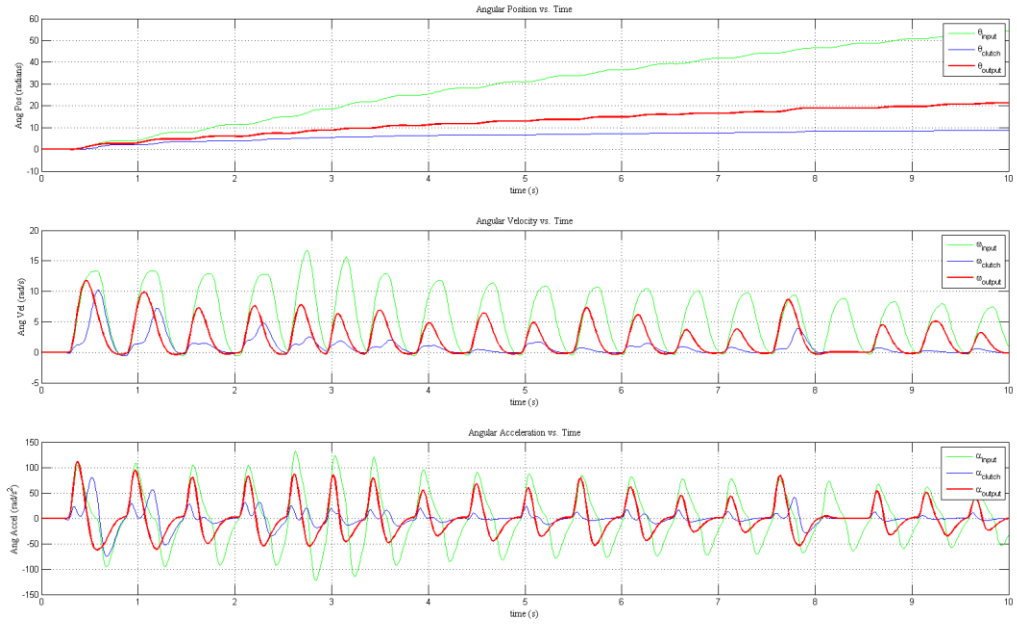

Figure 49: Cam Spring Data Set 1.10

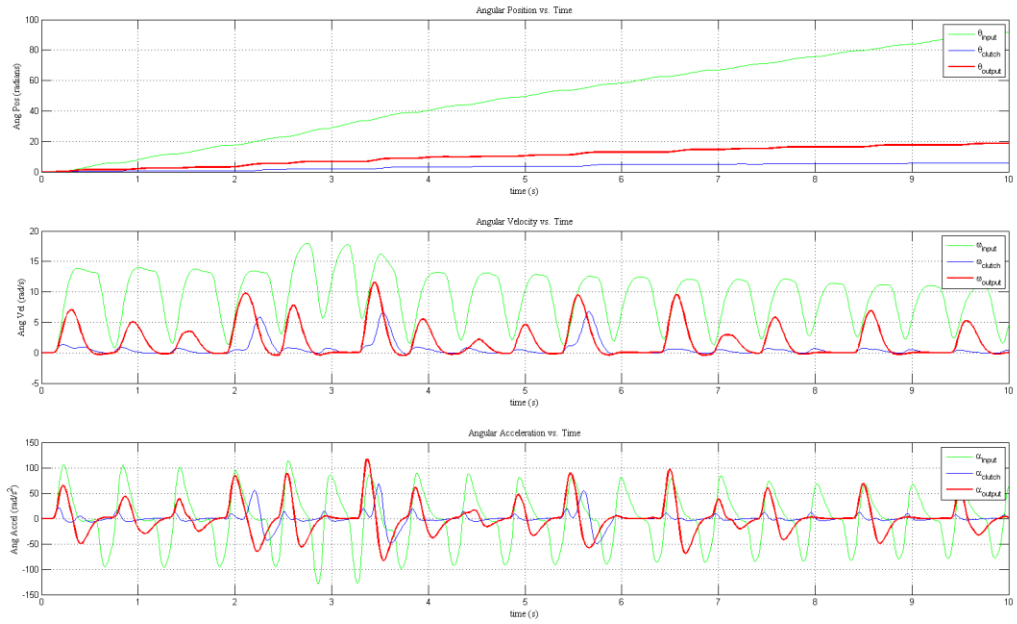

Figure 50: Cam Spring Data Set 1.11

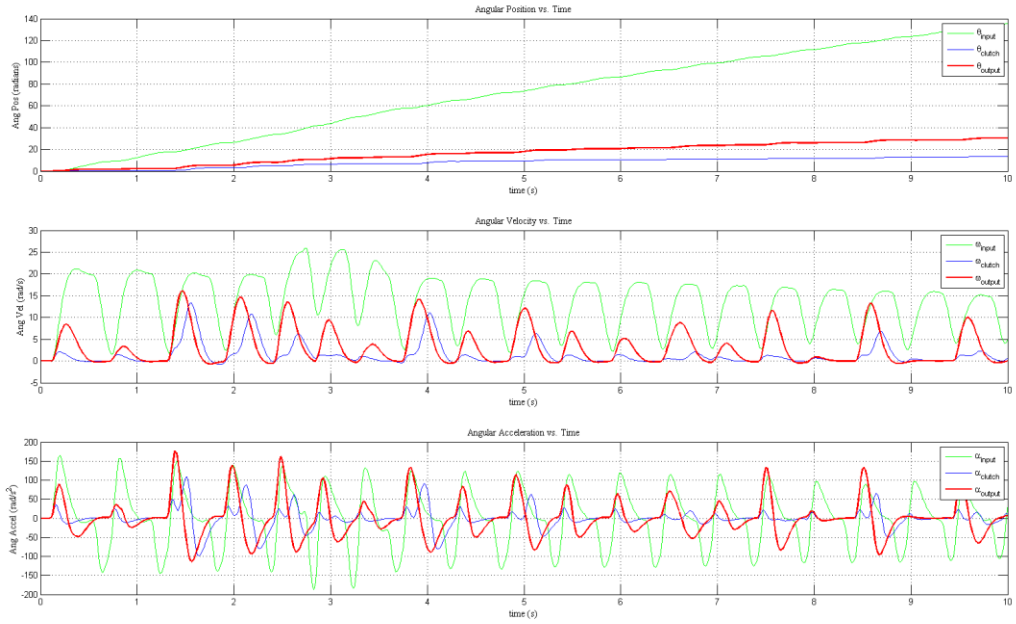

Figure 51: Cam Spring Data Set 1.12

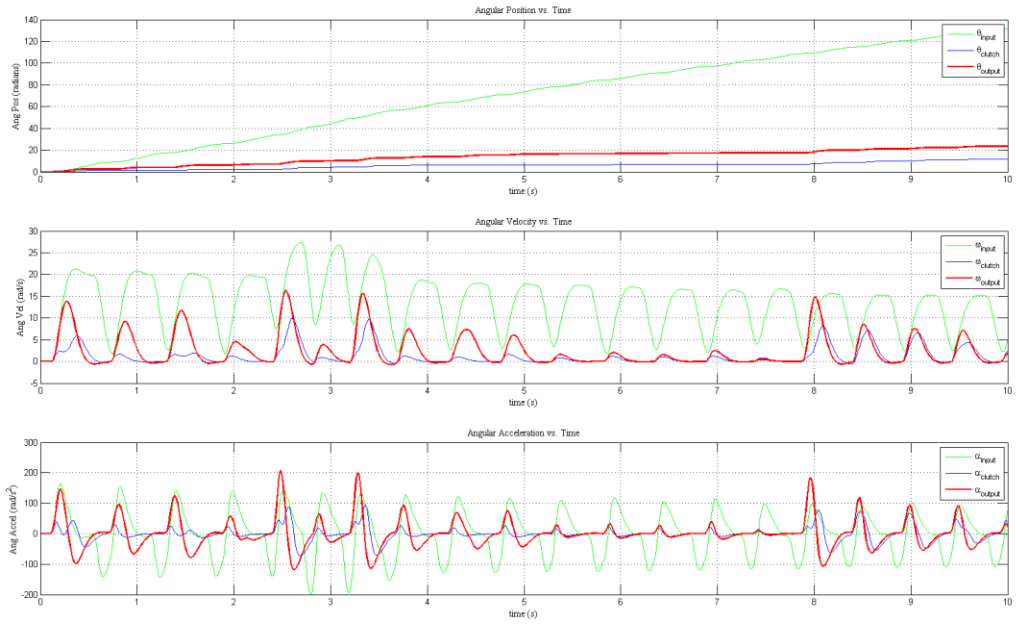

Figure 52: Cam Spring Data Set 1.13

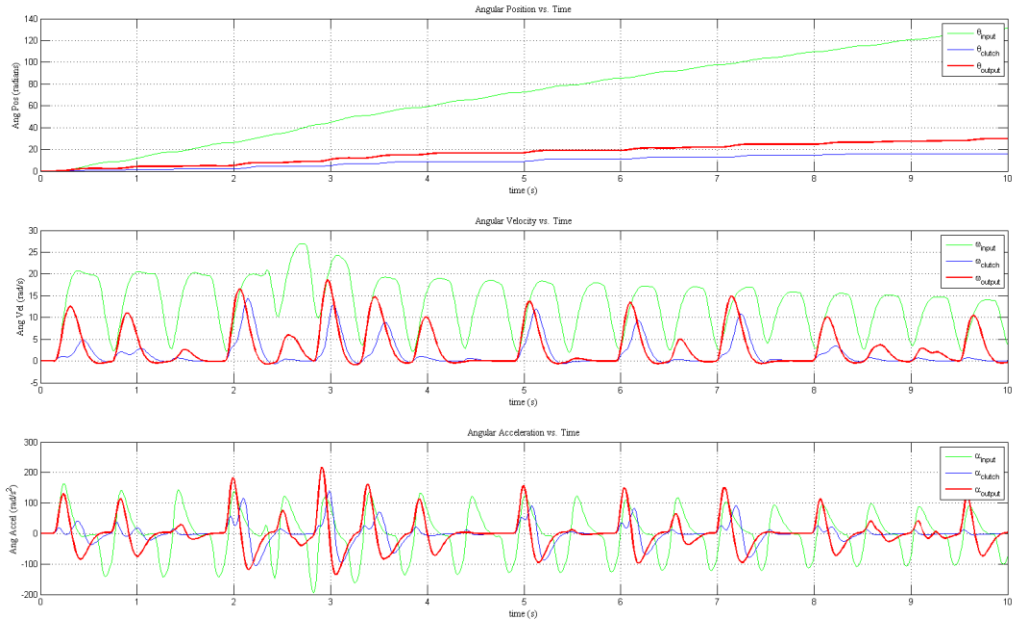

Figure 53: Cam Spring Data Set 1.14

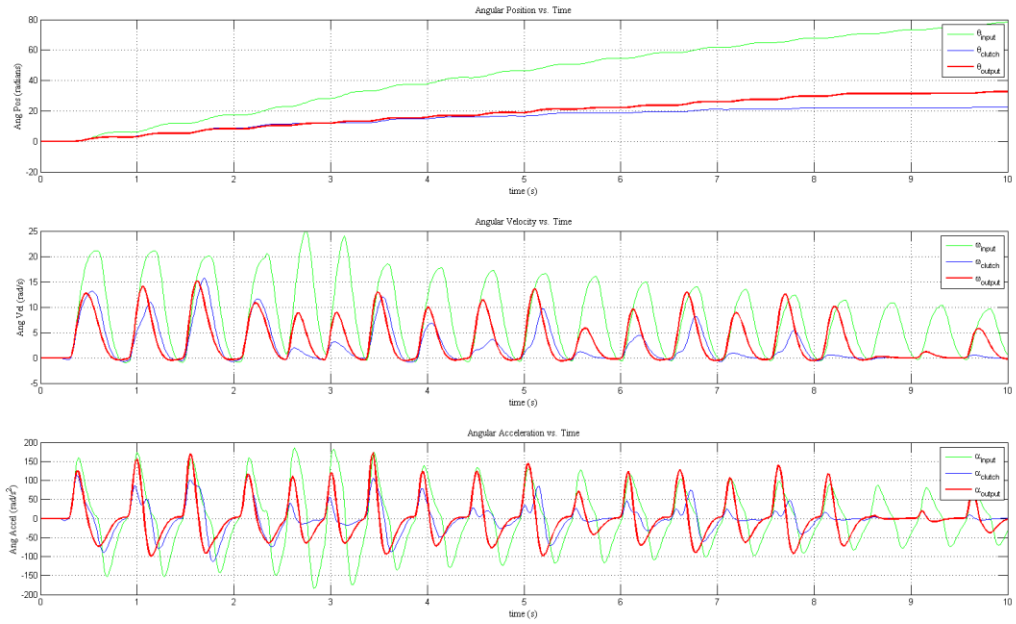

Figure 54: Cam Spring Data Set 1.15

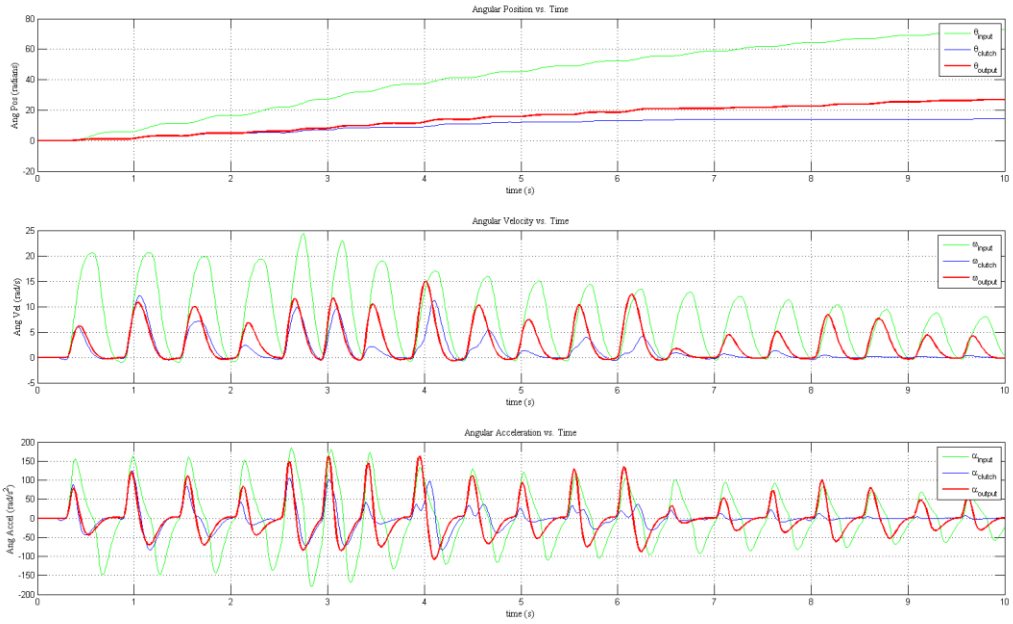

Figure 55: Cam Spring Data Set 1.16

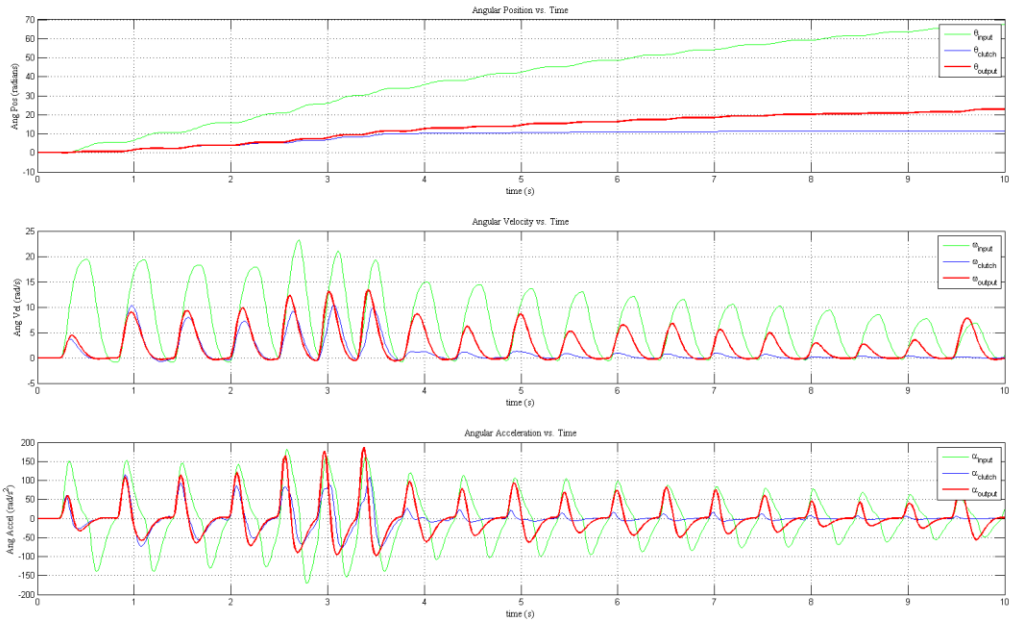

Figure 56: Cam Spring Data Set 1.17

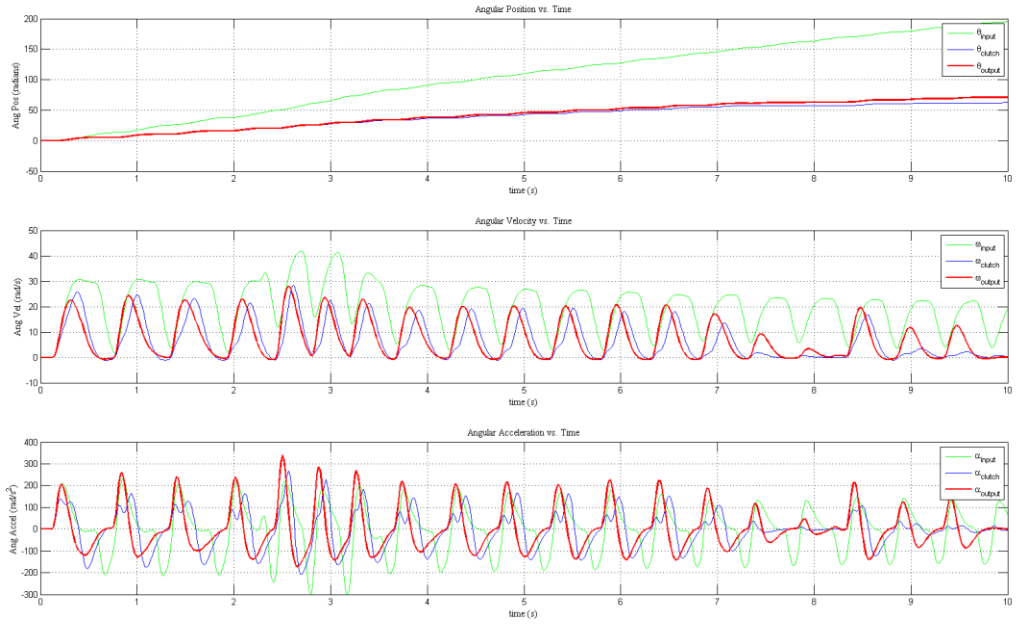

Figure 57: Cam Spring Data Set 1.18

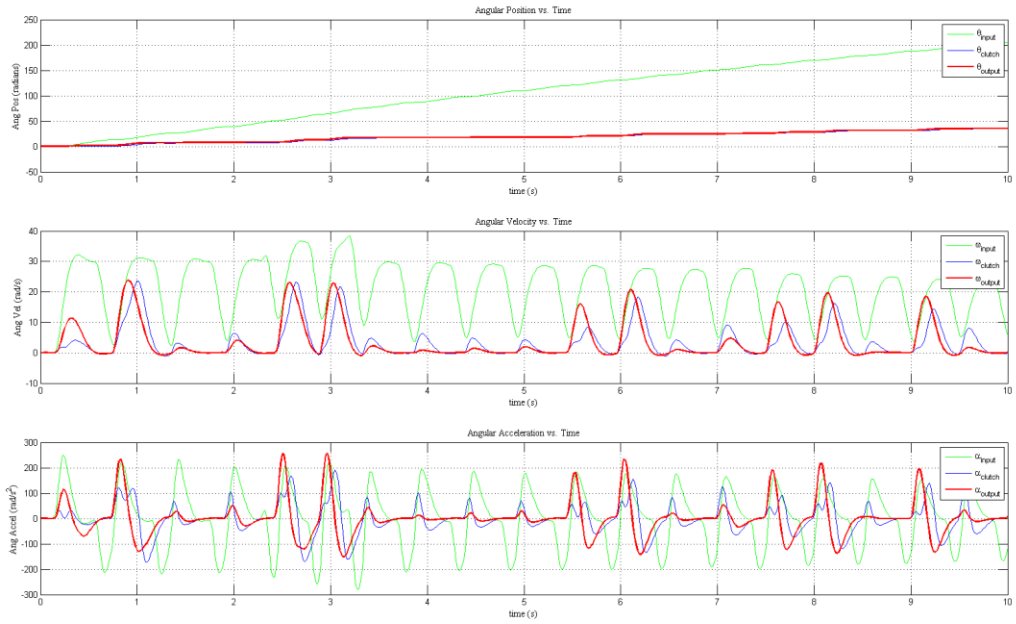

Figure 58: Cam Spring Data Set 1.19

Series Spring

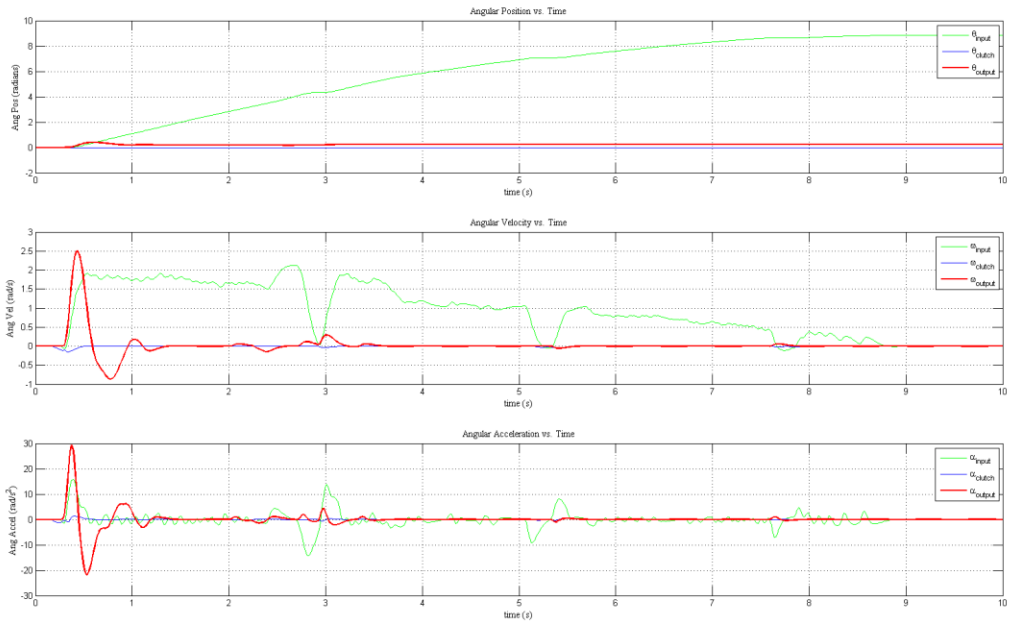

Figure 59: Series Spring Data Set 1.1

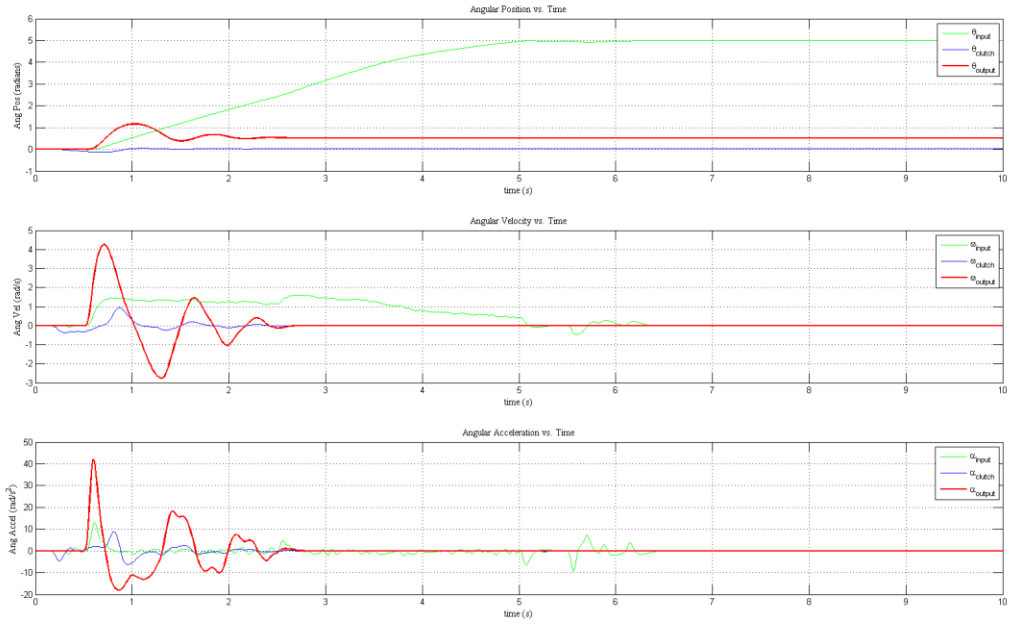

Figure 60: Series Spring Data Set 1.2

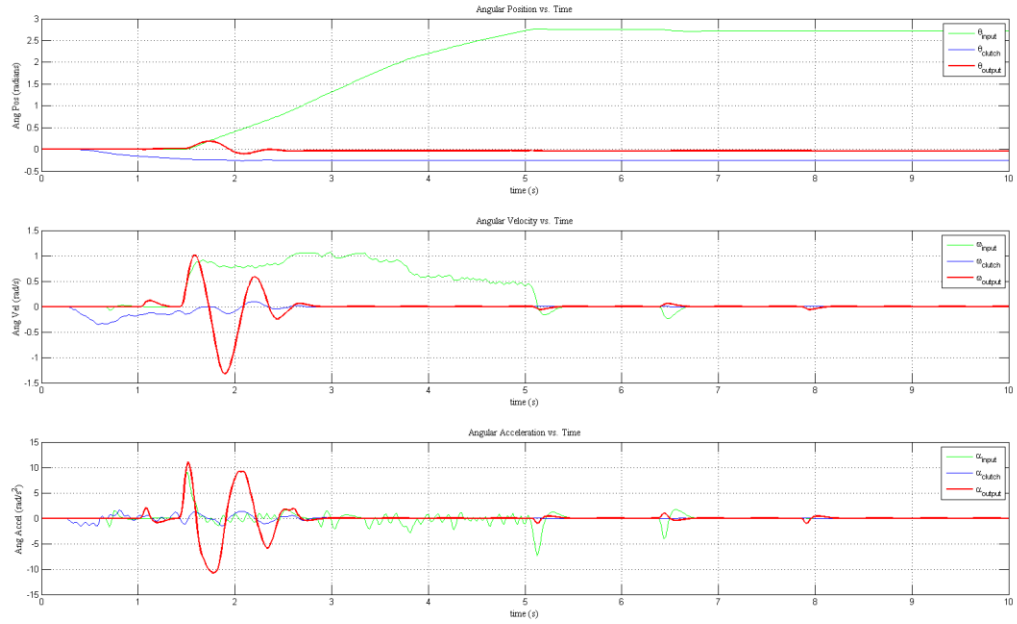

Figure 61: Series Spring Data Set 1.3

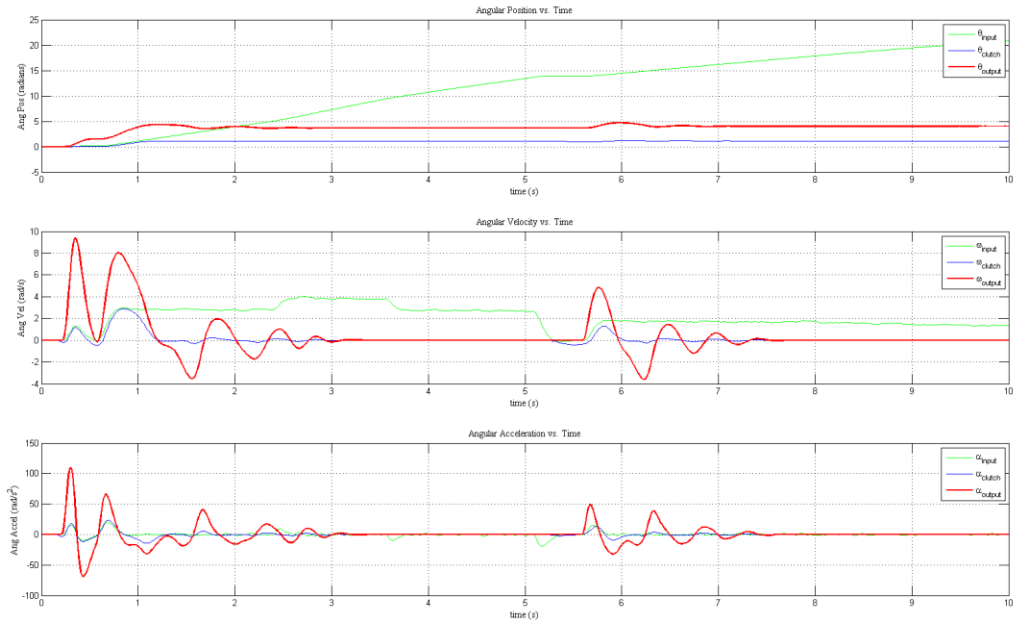

Figure 62: Series Spring Data Set 1.4

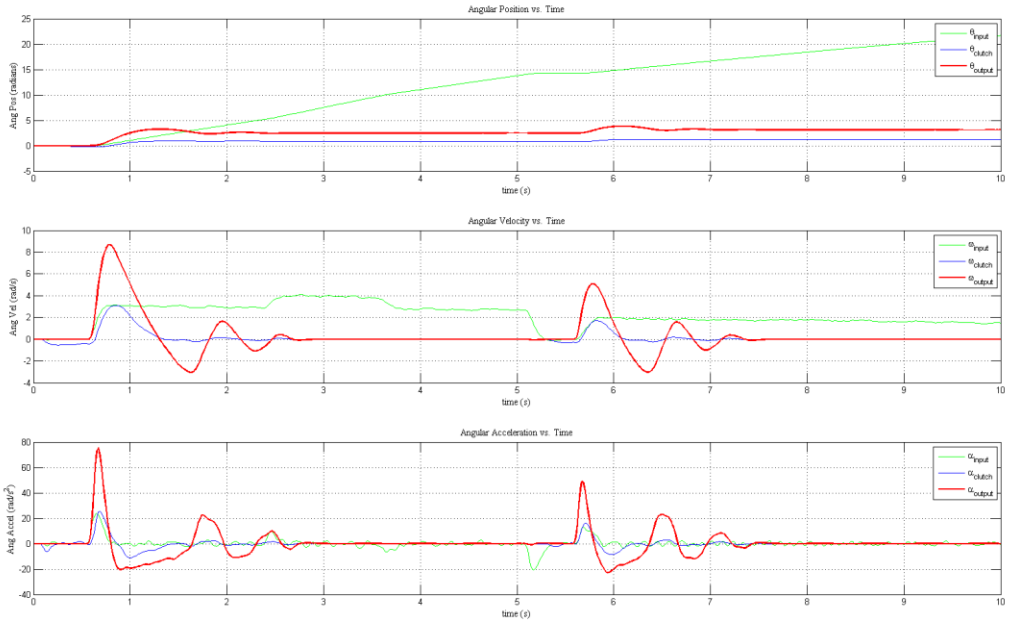

Figure 63: Series Spring Data Set 1.5

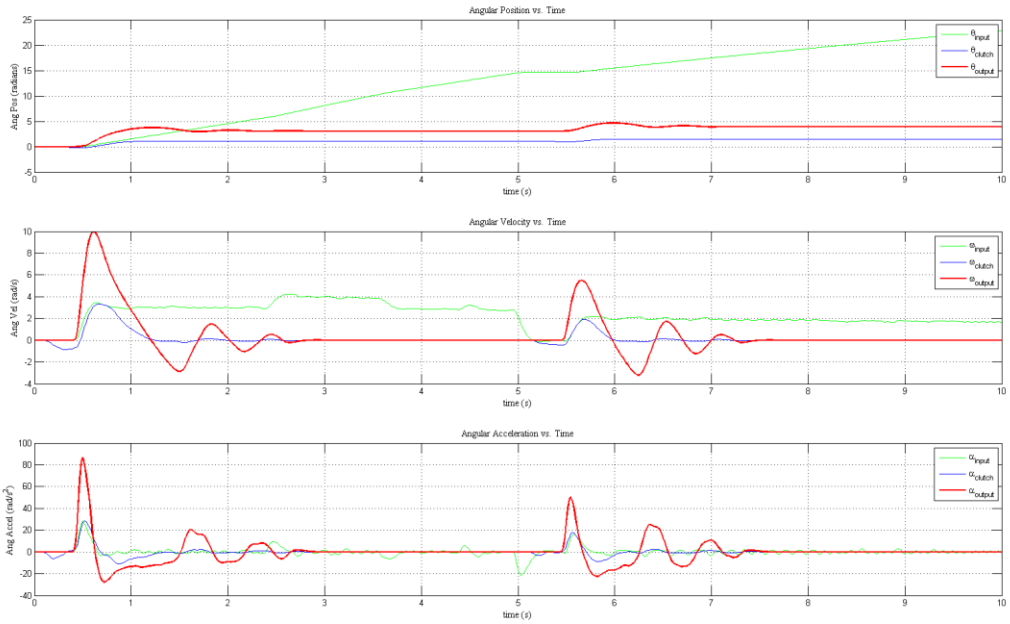

Figure 64: Series Spring Data Set 1.6

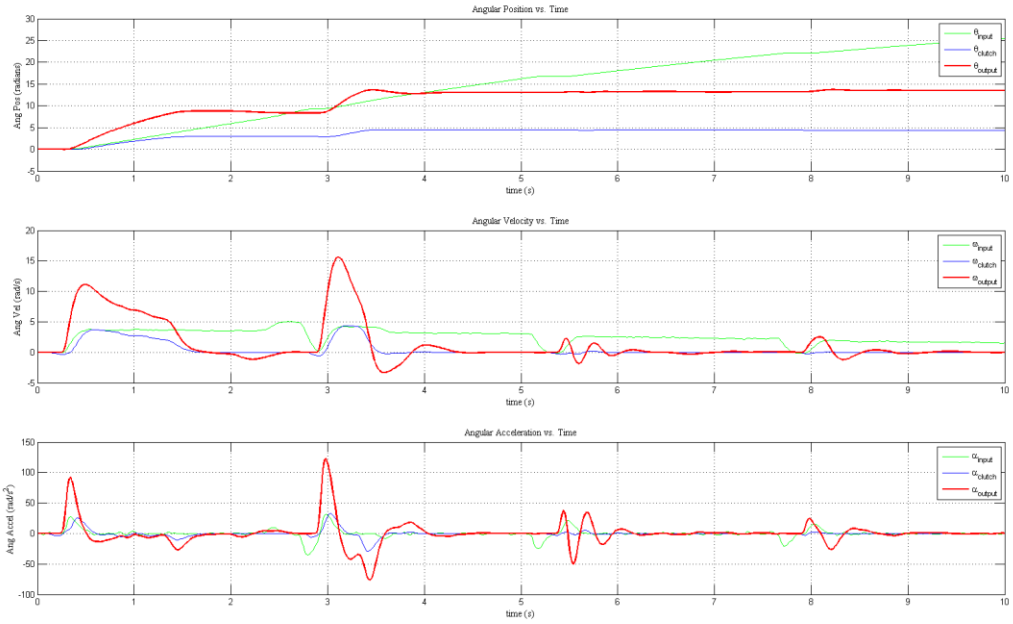

Figure 65: Series Spring Data Set 1.7

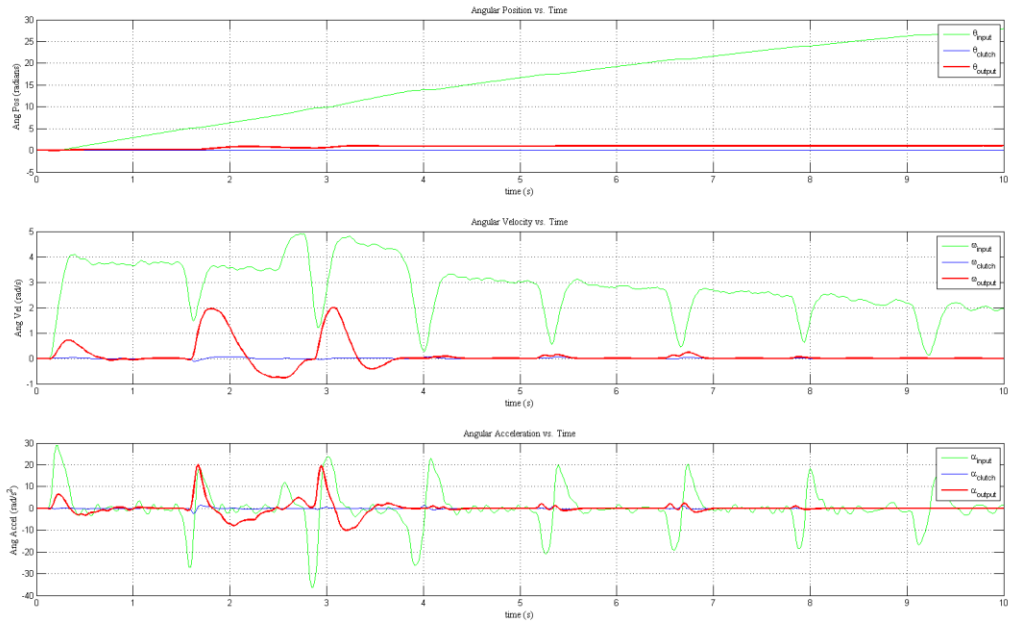

Figure 66: Series Spring Data Set 1.8

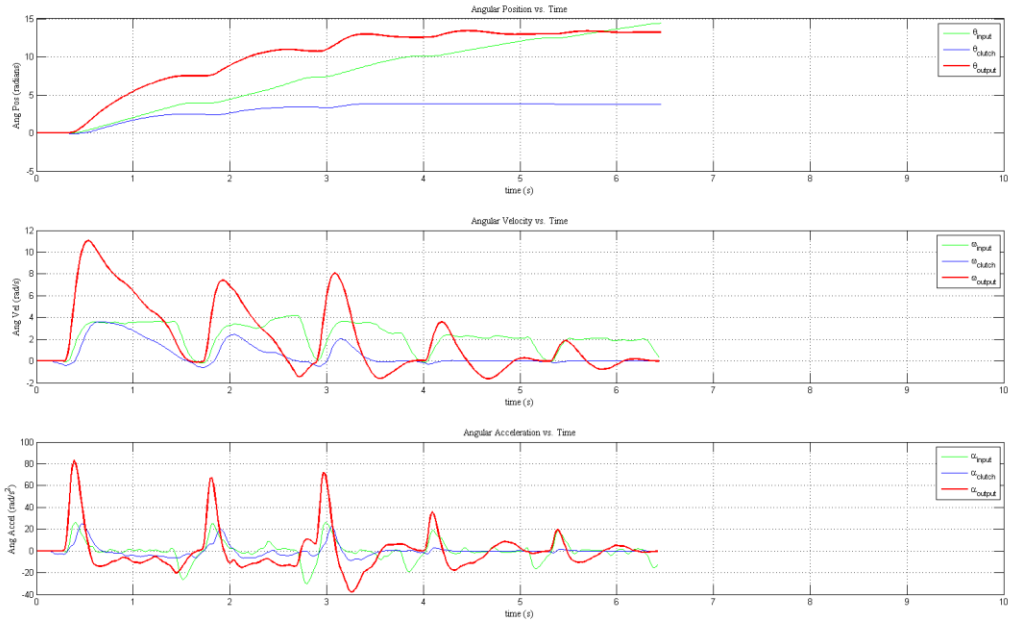

Figure 67: Series Spring Data Set 1.9

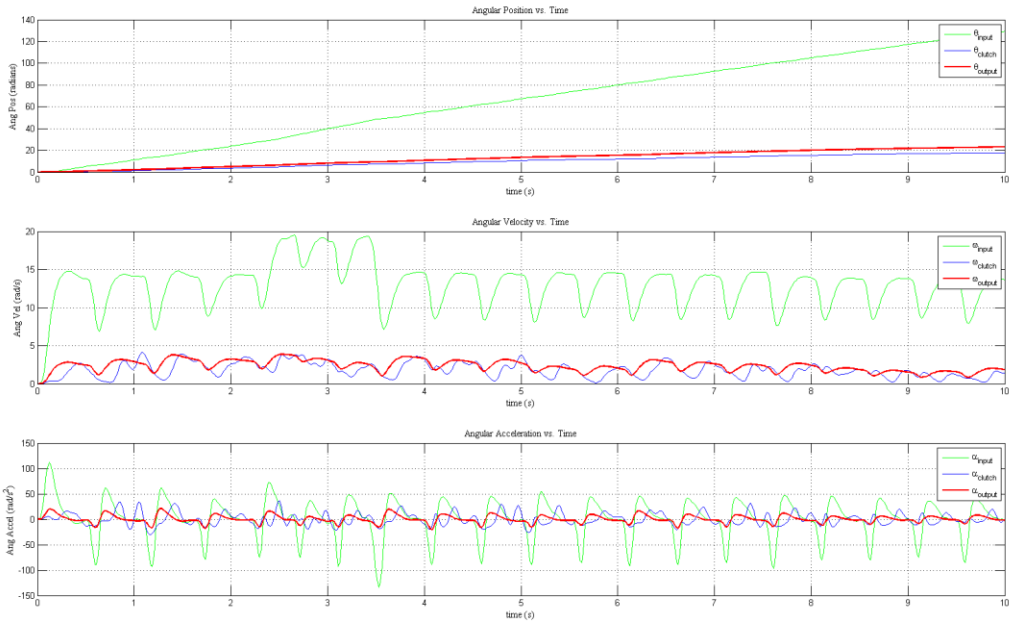

Figure 68: Series Spring Data Set 1.10

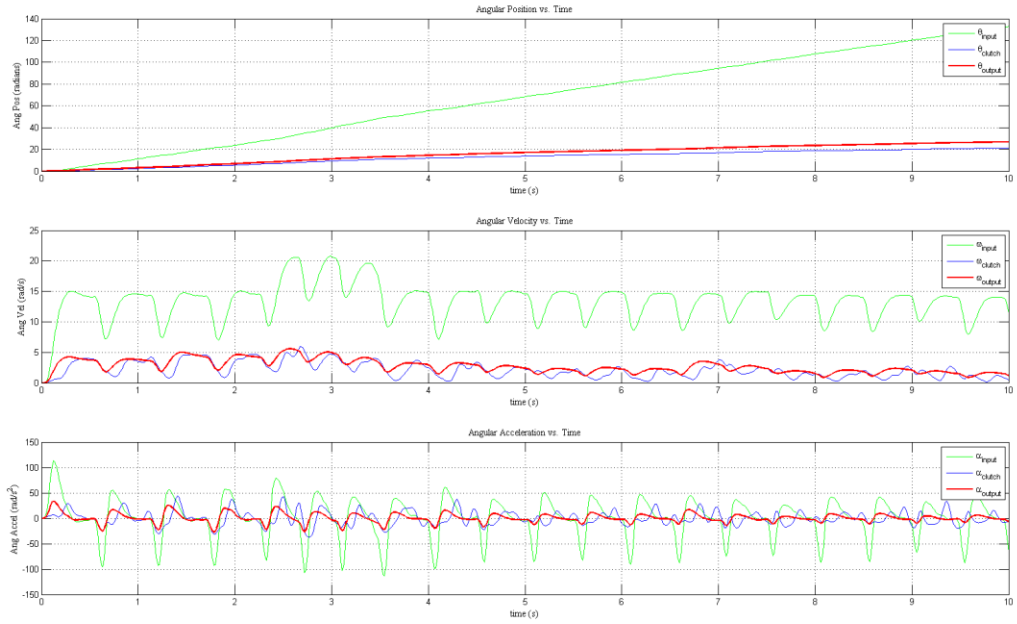

Figure 69: Series Spring Data Set 1.11

Appendix B – Round 2 Plots

The following section contains the angular displacement, velocity, and acceleration graphs that were generated for each test performed on the Cam Spring during Round 2 testing. For an explanation of how these plots were derived, see Round 1 - Quantitative Results.

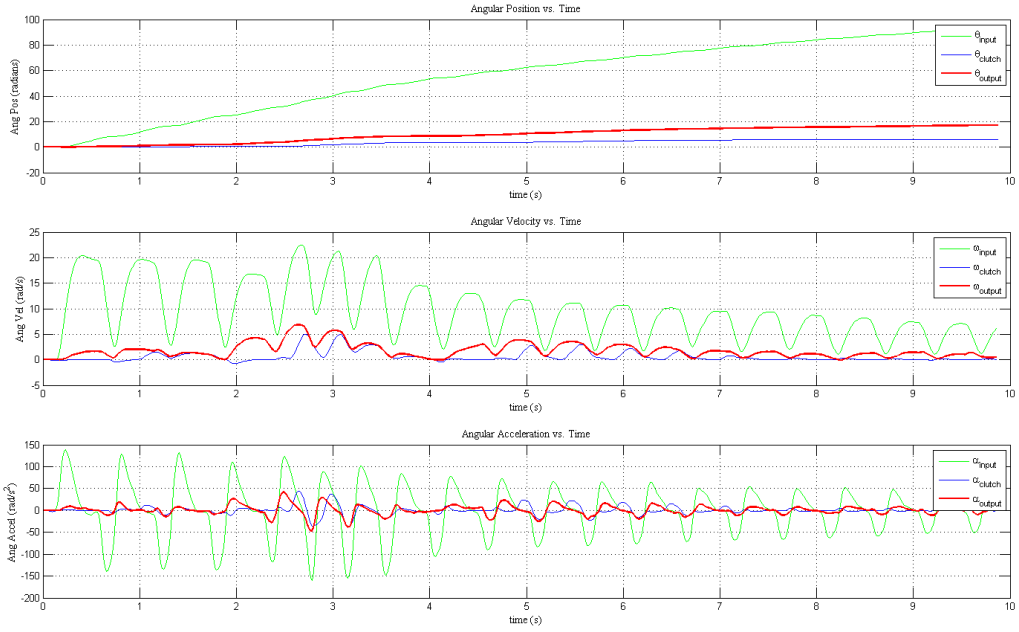

Figure 70: Cam Spring Data Set 2.1

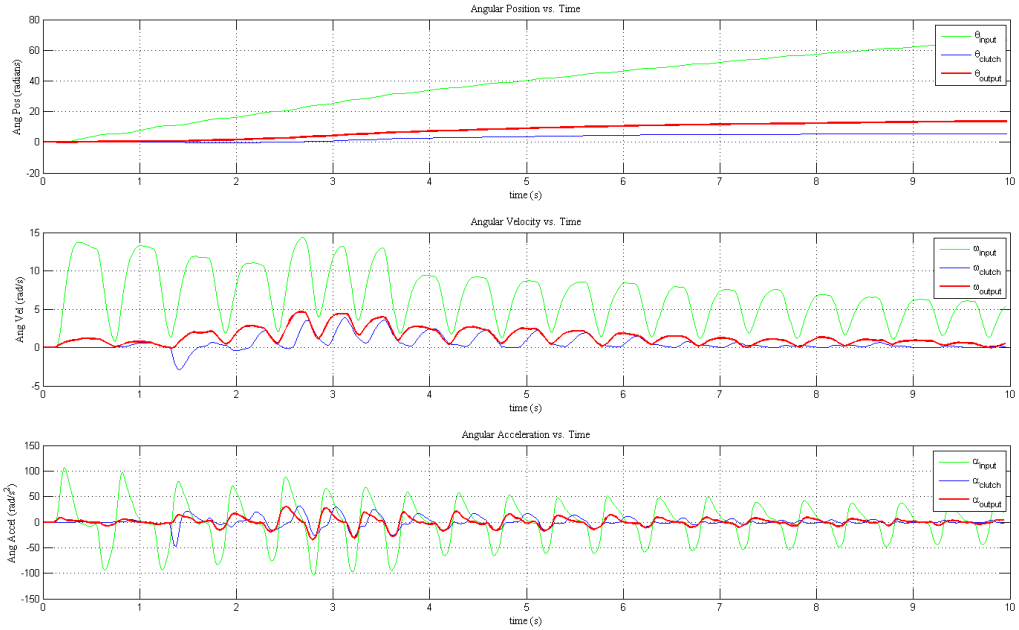

Figure 71: Cam Spring Data Set 2.2

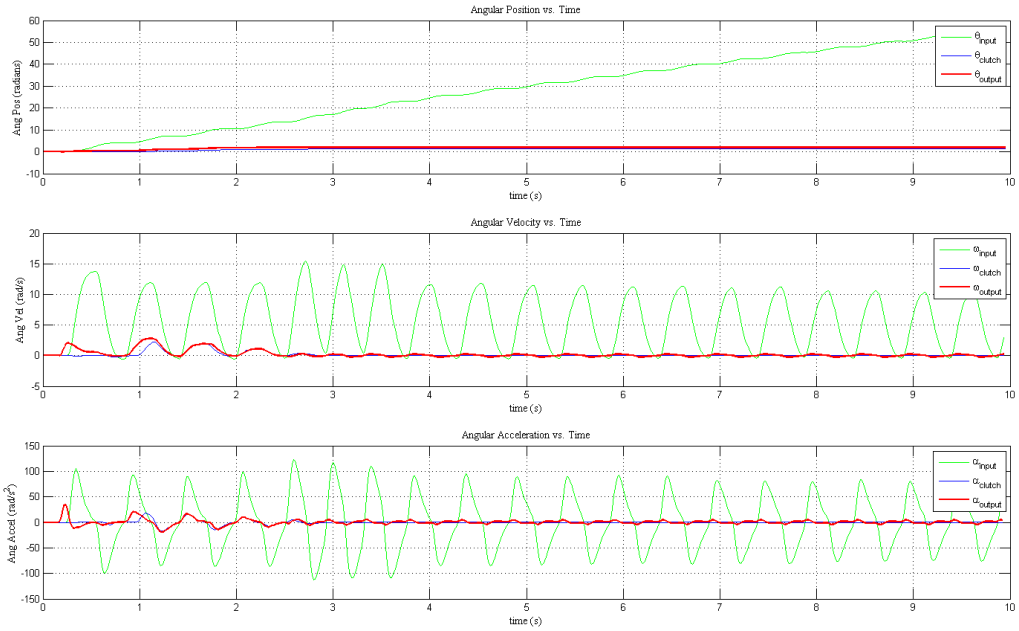

Figure 72: Series Spring Data Set 2.3

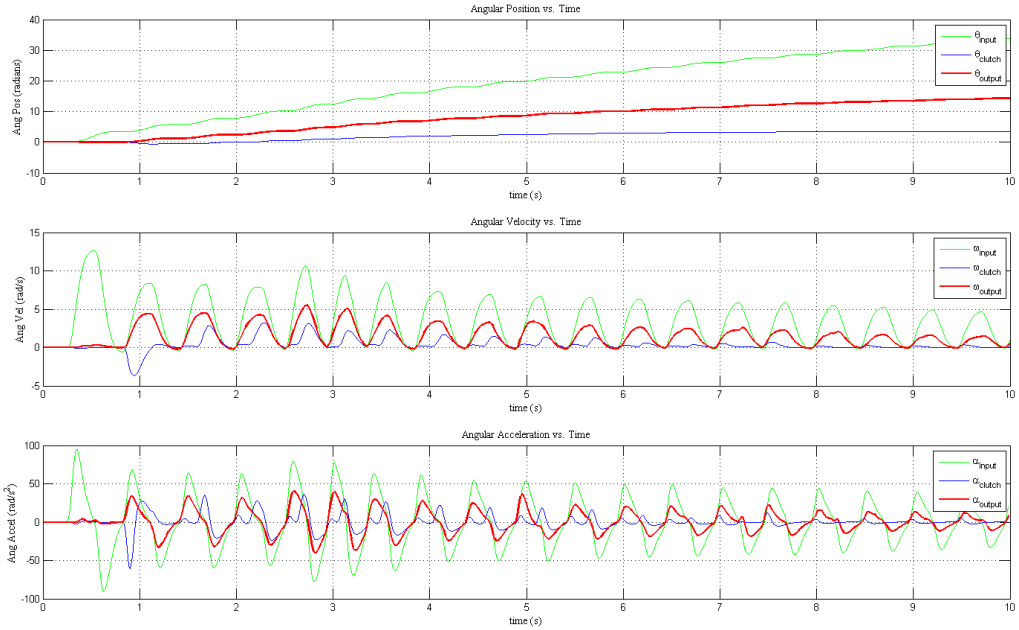

Figure 73: Cam Spring Data Set 2.4

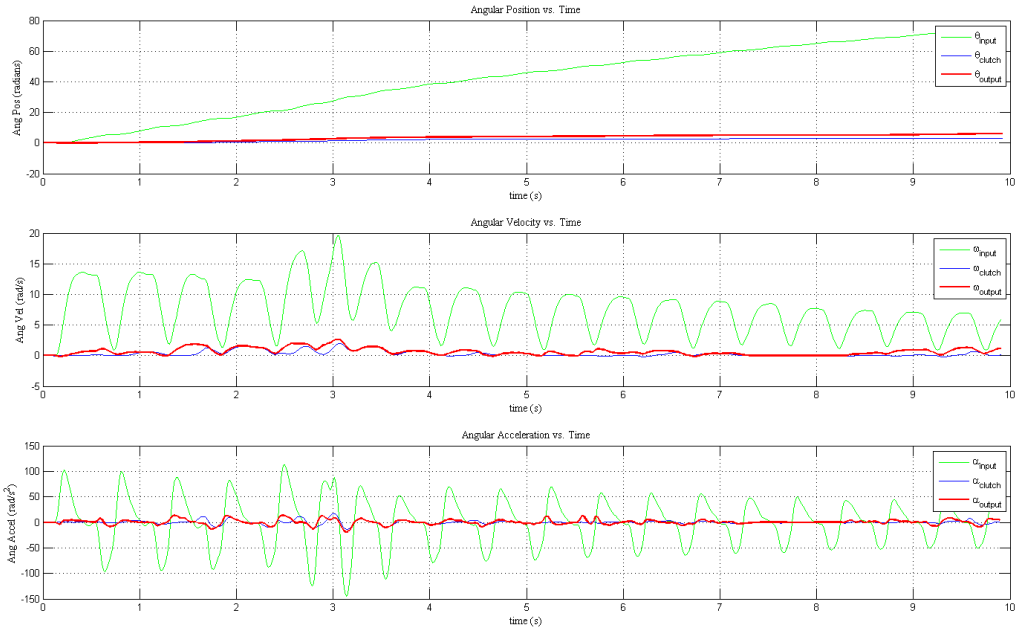

Figure 74: Cam Spring Data Set 2.5

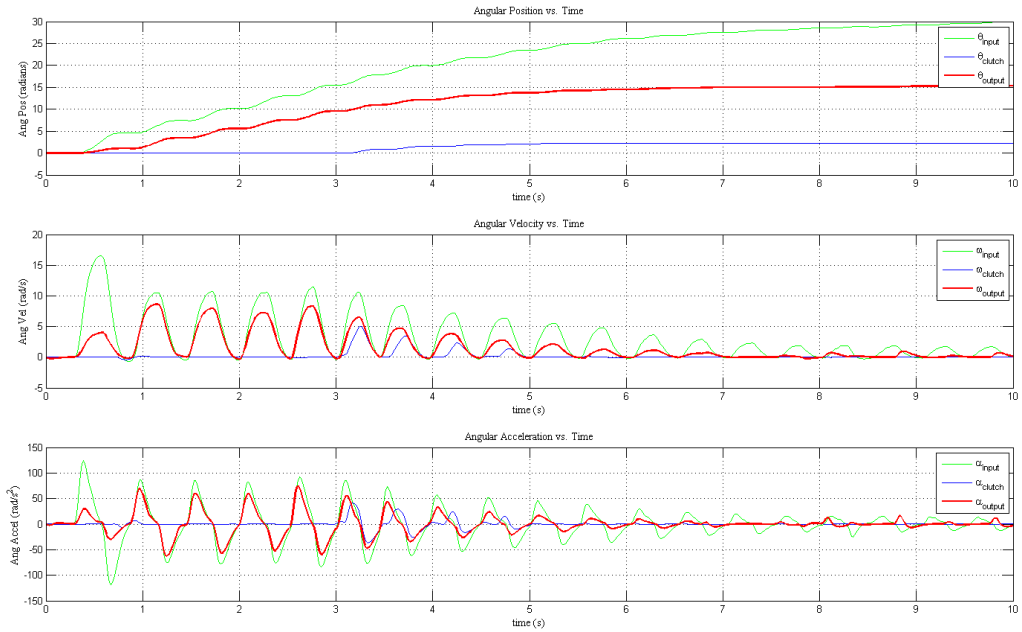

Figure 75: Cam Spring Data Set 2.6

Appendix C – Photo Documentation

The following section contains images and videos taken by the group during testing of various aspects of the full test setup, including wiring, DAQ layout, and the test assembly.

Video documentation of the testing may be viewed on http://www.youtube.com/ under the channel name WPIMEPSCVT.

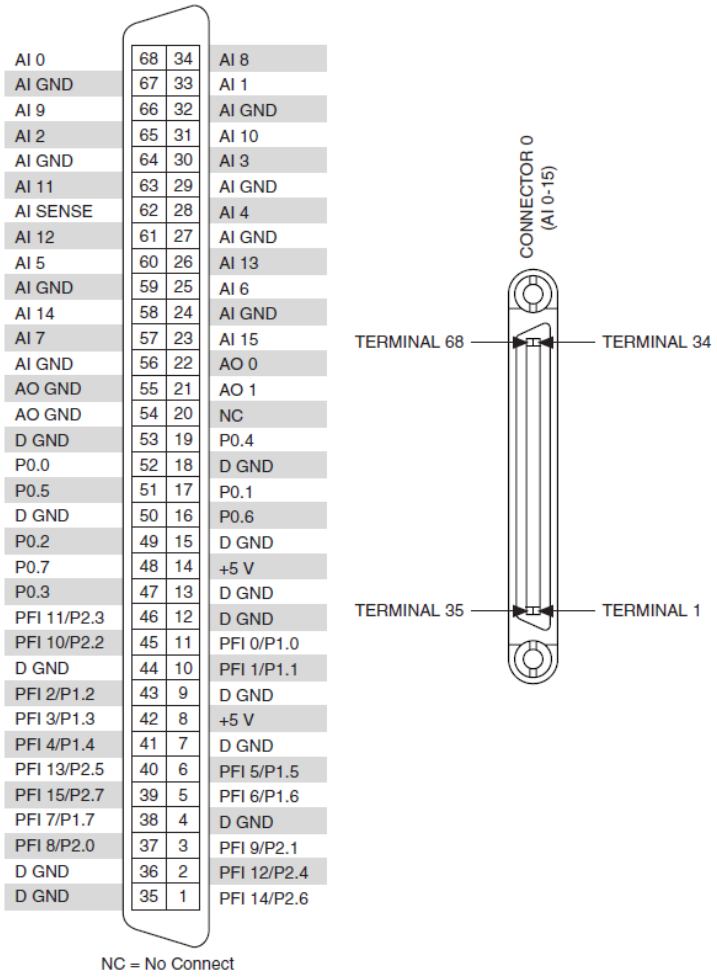

Figure 76: NI DAQ Pin Diagram

Table 3-2. NI 660x Connector Pin Assignments

Signal Name	Motion Encoder Context	DIO Context	Counter Context (Default)	Pin Number	Pin Number	Counter Context (Default)	DIO Context	Motion Encoder Context	Signal Name
PFI 31	channel A(2)	P0.31	CTR 2 SRC	34	68	—	—	—	D GND
D GND	—	—	—	33	67	CTR 2 GATE	P0.30	index/z(2)	PFI 30
PFI 28	—	P0.28	CTR 2 OUT	32	66	CTR 2 AUX	P0.29	channel B(2)	PFI 29
PFI 27	channel A(3)	P0.27	CTR 3 SRC	31	65	—	—	—	D GND
D GND	—	—	—	30	64	CTR 3 GATE	P0.26	index/z(3)	PFI 26
PFI 24	—	P0.24	CTR 3 OUT	29	63	CTR 3 AUX	P0.25	channel B(3)	PFI 25
PFI 23	channel A(4)	P0.23	CTR 4 SRC	28	62	—	—	—	D GND
D GND	—	—	—	27	61	CTR 4 GATE	P0.22	index/z(4)	PFI 22
PFI 20	—	P0.20	CTR 4 OUT	26	60	CTR 4 AUX	P0.21	channel B(4)	PFI 21
PFI 19	channel A(5)	P0.19	CTR 5 SRC	25	59	—	—	—	D GND
D GND	—	—	—	24	58	CTR 5 GATE	P0.18	index/z(5)	PFI 18
PFI 16	—	P0.16	CTR 5 OUT	23	57	CTR 5 AUX	P0.17	channel B(5)	PFI 17
PFI 15	channel A(6)	P0.15	CTR 6 SRC	22	56	—	—	—	RG
PFI 14	index/z(6)	P0.14	CTR 6 GATE	21	55	—	—	—	D GND
D GND	—	—	—	20	54	CTR 6 AUX	P0.13	channel B(6)	PFI 13
RG	—	—	—	19	53	CTR 6 OUT	P0.12	—	PFI 12
D GND	—	—	—	18	52	CTR 7 SRC	P0.11	channel A(7)	PFI 11

Signal Name	Motion Encoder Context	DIO Context	Counter Context (Default)	Pin Number	Pin Number	Counter Context (Default)	DIO Context	Motion Encoder Context	Signal Name
PFI 9	channel B(7)	P0.9	CTR 7 AUX	17	51	CTR 7 GATE	P0.10	index/z(7)	PFI 10
PFI 8	—	P0.8	CTR 7 OUT	16	50	—	—	—	D GND
PFI 7	—	P0.7	—	15	49	—	—	—	D GND
D GND	—	—	—	14	48	—	P0.6	—	PFI 6
PFI 4	—	P0.4	—	13	47	—	P0.5	—	PFI 5
PFI 3	—	P0.3	—	12	46	—	—	—	D GND
D GND	—	—	—	11	45	—	P0.2	—	PFI 2
PFI 0	—	P0.0	—	10	44	—	P0.1	—	PFI 1
PFI 32	—	—	CTR 1 OUT	9	43	—	—	—	RG
PFI 34	index/z(1)	—	CTR 1 GATE	8	42	—	—	—	D GND
PFI 35	channel A(1)	—	CTR 1 SRC	7	41	—	—	—	D GND
PFI 33	channel B(1)	—	CTR 1 AUX	6	40	CTR 0 AUX	—	channel B(0)	PFI 37
PFI 36	—	—	CTR 0 OUT	5	39	—	—	—	D GND
Reserved	—	—	—	4	38	—	—	—	Reserved
PFI 38	index/z(0)	—	CTR 0 GATE	3	37	—	—	—	Reserved
PFI 39	channel A(0)	—	CTR 0 SRC	2	36	—	—	—	GND
+5 V	—	—	—	1	35	—	—	—	RG

Figure 77: Counter Pin Location List (Used to Wire encoders)

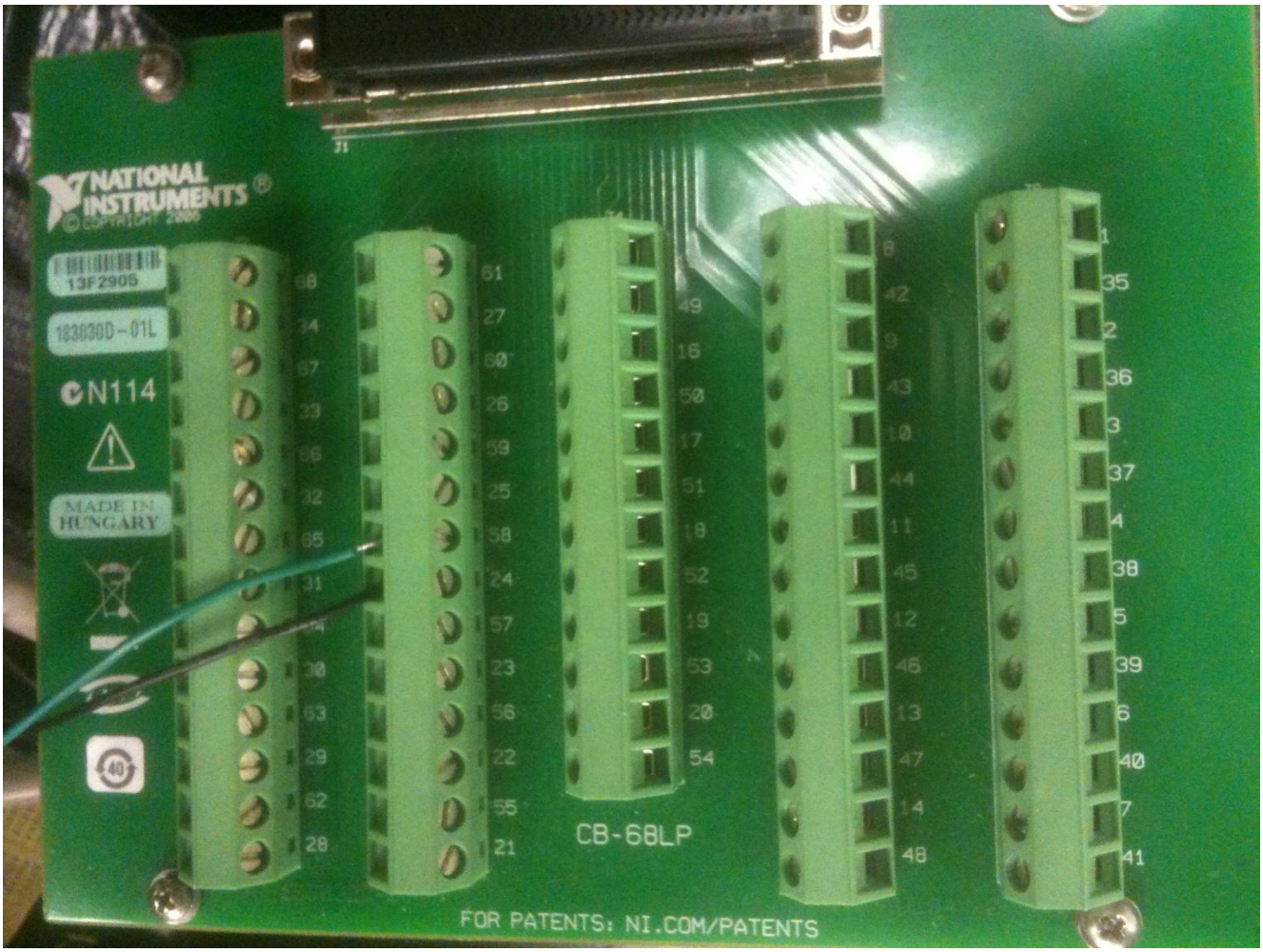

Figure 78: NI PCI-6220 Wiring Photo (Hall Effect Sensor)

PCI- 6220
Ai14-58
AIGND-24

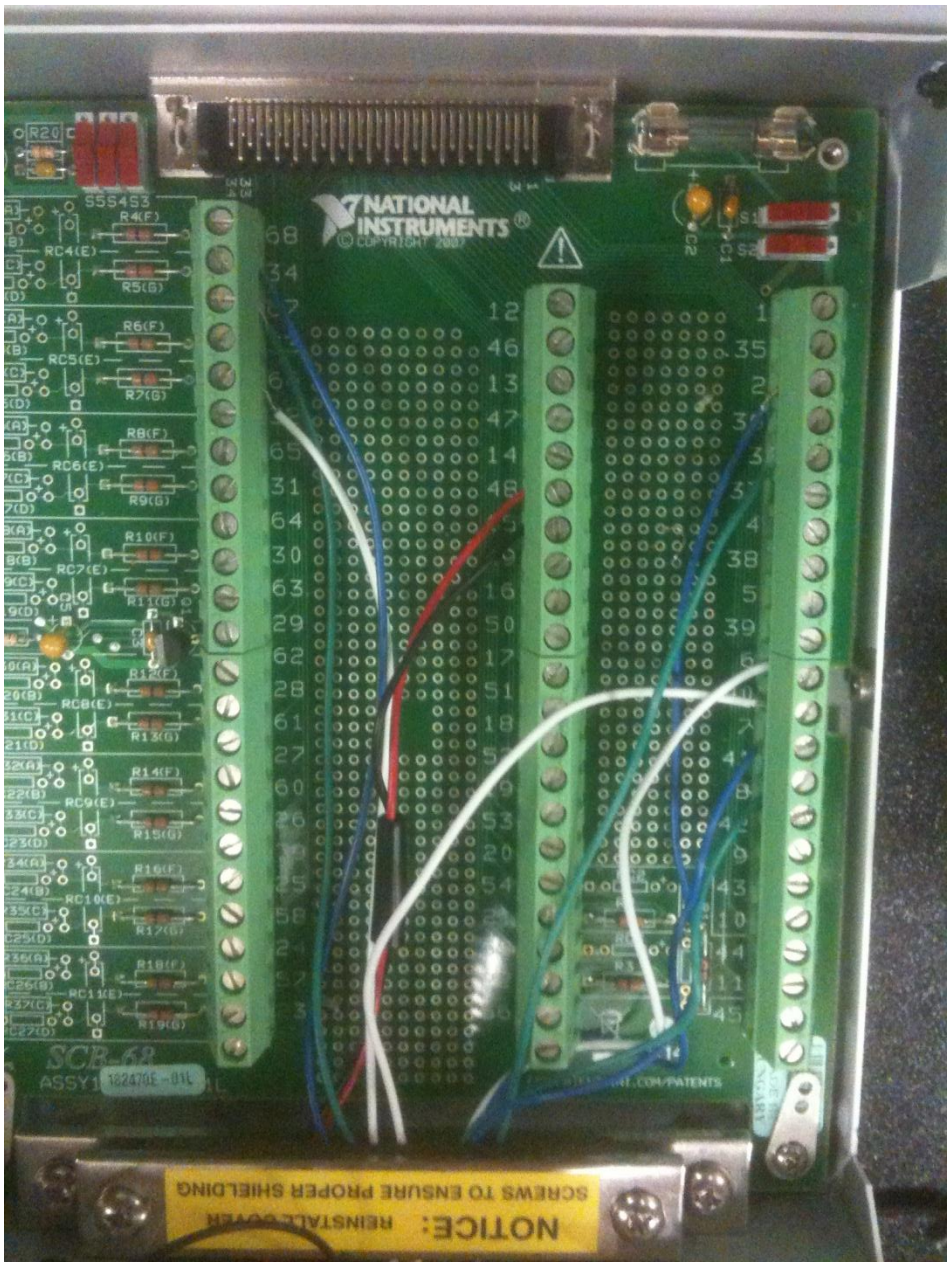

Figure 79: NI PCI 6024E Wiring Photo (Encoders)

PCI 6601
PFI39/Gate0-2-A channel (Encoder B)
PFI 39/Source0-3-Index (Encoder B)
PFI37/UP_Down0-40-B channel (Encoder B)
PFI33/UP_Down1-6-B channel (Encoder A)
PFI35/Source1-7-A channel (Encoder A)
PFI34/Gate1-8-Index (Encoder A)
PFI6/DIO2-48-Power +
PFI7/DIO7-15-Ground

PFI31/Source2-34-A channel (Encoder C)
PFI30/Gate2-67-Index (Encoder C)
PFI28/UP_Down2-66-B channel (Encoder C)

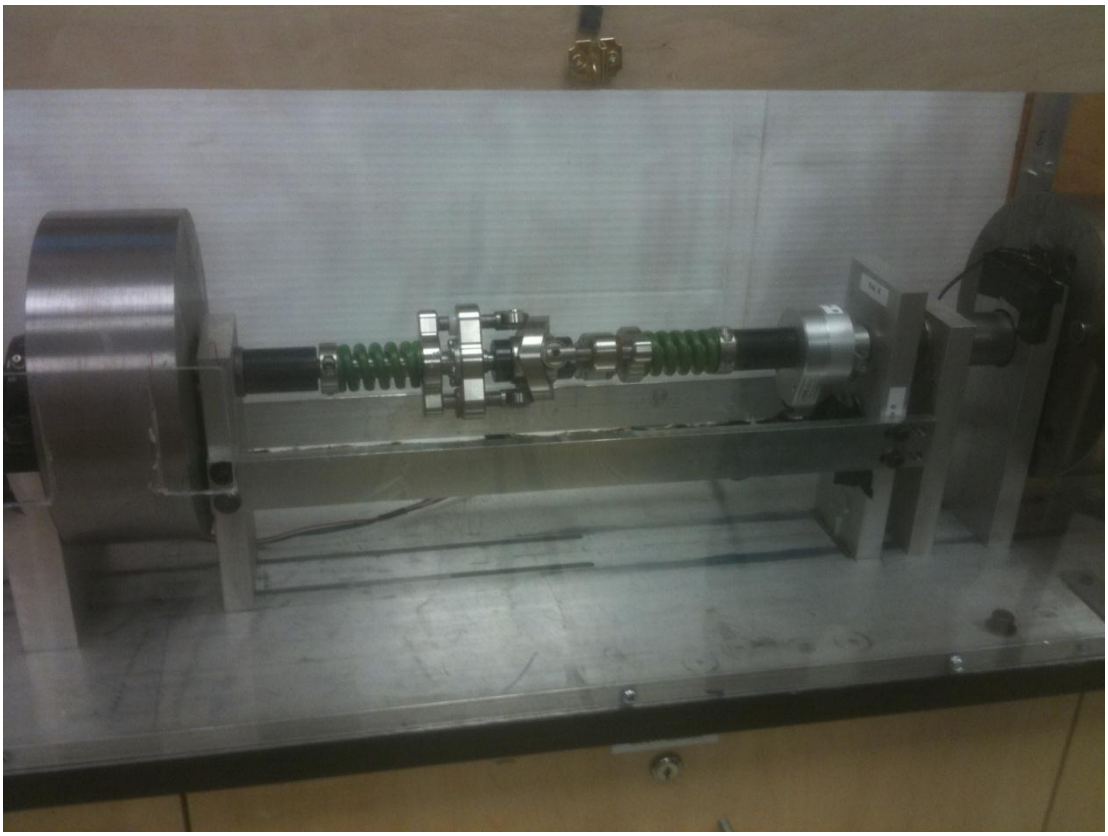

Figure 80: Final Testing Assembly